

Effects of ice particle size vertical inhomogeneity on the passive remote sensing of ice clouds

Zhibo Zhang,¹ Steven Platnick,² Ping Yang,³ Andrew K. Heidinger,⁴ and Jennifer M. Comstock⁵

Received 11 January 2010; revised 16 April 2010; accepted 27 April 2010; published 3 September 2010.

[1] The solar reflectance bi-spectral (SRBS) and infrared split-window (IRSpW) methods are two of the most popular techniques for passive ice cloud property retrievals from multispectral imagers. Ice clouds are usually assumed to be vertically homogeneous in global operational algorithms based on these methods, although significant vertical variations of ice particle size are typically observed in ice clouds. In this study we investigate uncertainties in retrieved optical thickness, effective particle size, and ice water path introduced by a homogeneous cloud assumption in both the SRBS and IRSpW methods, and focus on whether the assumption can lead to significant discrepancies between the two methods. The study simulates the upwelling spectral radiance associated with vertically structured clouds and passes the results through representative SRBS and IRSpW retrieval algorithms. Cloud optical thickness is limited to values for which IRSpW retrievals are possible (optical thickness less than about 7). When the ice cloud is optically thin and yet has a significant ice particle size vertical variation, it is found that both methods tend to underestimate the effective radius and ice water path. The reason for the underestimation is the nonlinear dependence of ice particle scattering properties (extinction and single scattering albedo) on the effective radius. Because the nonlinearity effect is stronger in the IRSpW than the SRBS method, the IRSpW-based IWP tends to be smaller than the SRBS counterpart. When the ice cloud is moderately optically thick, the IRSpW method is relatively insensitive to cloud vertical structure and effective radius retrieval is weighted toward smaller ice particle size, while the weighting function makes the SRBS method more sensitive to the ice particle size in the upper portion of the cloud. As a result, when ice particle size increases monotonically toward cloud base, the two methods are in qualitative agreement; in the event that ice particle size decreases toward cloud base, the effective radius and ice water path retrievals based on the SRBS method are substantially larger than those from the IRSpW. The main findings of this study suggest that the homogenous cloud assumption can affect the SRBS and IRSpW methods to different extents and, consequently, can lead to significantly different retrievals. Therefore caution should be taken when comparing and combining the ice cloud property retrievals from these two methods.

Citation: Zhang, Z., S. Platnick, P. Yang, A. K. Heidinger, and J. M. Comstock (2010), Effects of ice particle size vertical inhomogeneity on the passive remote sensing of ice clouds, *J. Geophys. Res.*, 115, D17203, doi:10.1029/2010JD013835.

¹Goddard Earth Science and Technology Center, University of Maryland, Baltimore County, Baltimore, Maryland, USA.

²Laboratory for Atmospheres, NASA Goddard Space Flight Center, Greenbelt, Maryland, USA.

³Department of Atmospheric Sciences, Texas A&M University, College Station, Texas, USA.

⁴Center for Satellite Applications and Research, NOAA National Environmental Satellite, Data, and Information Service, Madison, Wisconsin, USA.

⁵Pacific Northwest National Laboratory, Richland, Washington, USA.

1. Introduction

[2] Although the significant role of ice clouds in the climate system has long been recognized [Liou, 1986; Ramanathan *et al.*, 1989; Hartmann *et al.*, 1992], a complete understanding of this role has not yet been achieved. The current generation of general circulation models (GCM) still exhibits a large range in ice cloud radiative forcing estimates [Zhang *et al.*, 2005]. The differences in globally averaged ice water path (IWP) among the current generation of GCMs are estimated to be as large as an order of magnitude [Waliser *et al.*, 2009]. As a result, significant uncertainties remain in the climatology of ice cloud prop-

erties and the response and feedback of these clouds to anthropogenic radiative forcing [Webb *et al.*, 2006]. In order to improve our understanding of ice clouds, particularly their potential feedbacks to global warming, long-term, global satellite-based observations of ice cloud properties are indispensable. However, as shown by many studies [e.g., Waliser *et al.*, 2009; Zhang *et al.*, 2009], different observational techniques and/or different assumptions about ice cloud microphysics can lead to substantially different retrievals. Therefore, as we continue to improve the capabilities of satellite sensors for ice cloud observations, it is also important to identify and explain differences among existing retrievals, so that long-term, consistent climatologies of global ice cloud properties can be established.

[3] Among others, the cloud effective radius (r_e) and optical thickness (τ_c) are the two most fundamental microphysical and radiative parameters for ice clouds. The two largely determine the net radiative forcing [e.g., Ackerman *et al.*, 1988; Fu and Liou, 1993; Jensen *et al.*, 1994] and are closely related to the IWP. For these reasons, many satellite retrieval algorithms focus on the retrieval of τ_c and r_e . Among others, the bispectral solar reflectance method [Nakajima and King, 1990] and the infrared split-window method [Inoue, 1985, 1987; Prabhakara *et al.*, 1988; Ackerman *et al.*, 1990] have been extensively used for retrieving the τ_c and r_e from passive satellite multispectral imagers. Hereafter the two methods will be referred to as the “SRBS” and “IRSpW” methods, respectively. The SRBS method utilizes a pair of cloud reflection measurements, one usually in the visible (VIS) or near-infrared (NIR) spectral region and one in the shortwave or midwave infrared (SWIR and MWIR, respectively), to retrieve τ_c and r_e simultaneously. This method has been employed in cloud property retrieval algorithms for the Moderate Resolution Imaging Spectroradiometer (MODIS) [Platnick *et al.*, 2003], the Advanced Very High Resolution Radiometer (AVHRR) [Han *et al.*, 1994; Platnick and Twomey, 1994; Nakajima and Nakajima, 1995], and the Spinning Enhanced Visible and Infrared Imager (SEVIRI) [Roebeling *et al.*, 2006]. The future Visible Infrared Imaging Radiometer Suite (VIIRS) that will fly on the National Polar-Orbiting Environmental Satellite System (NPOESS) and on the NPOESS Preparatory Project (NPP) [Miller *et al.*, 2006] and the Advanced Baseline Imager planned to fly on the Geostationary Operational Environmental Satellite-R Series (GOES-R) [Schmit *et al.*, 2005] may also apply the SRBS method for their operational cloud retrievals. The IRSpW method relies on satellite measurements in the infrared atmospheric window region between about 8 to 13 μm for cloud property retrieval. With some variations, it has been applied for τ_c and r_e retrieval [e.g., Parol *et al.*, 1991; Strabala *et al.*, 1994; Huang *et al.*, 2004], as well as cloud detection [e.g., Ackerman *et al.*, 1998] and cloud thermodynamic phase determination [e.g., Ackerman *et al.*, 1990; Baum *et al.*, 2000]. The wide use of the SRBS and IRSpW methods has provided opportunities for cross comparison and evaluation of ice cloud property retrievals. It also seems feasible and promising to combine the two methods to derive long-term ice cloud climatologies, including both daytime and nighttime coverage, from multiple satellite platforms. However, it

is often found that the retrieved ice cloud properties based on different techniques are significantly different, even when they are applied to the same ice clouds [e.g., Comstock *et al.*, 2007; Zhang *et al.*, 2009]. Understanding the reasons for these differences is important, as it is the first step toward the integration of different techniques. Yet it is also a challenging task because numerous reasons can cause the two algorithm retrievals to differ.

[4] Among others, the vertical inhomogeneity of cloud particle size is an important factor that may lead to inconsistency between algorithms. Although most clouds have at least some degree of vertical inhomogeneity, cloud retrieval algorithms are usually based on a homogeneous cloud model. Cloud droplet size in nonprecipitating water clouds generally increases from cloud base to top as the air parcel rises through the cloud and more water is condensed [Martin *et al.*, 1994; Brenguier *et al.*, 2000; Miles *et al.*, 2000]. Most ice clouds, especially those that are synoptically driven, also have vertical structures. But different from water clouds, the sizes of ice particles in layered ice clouds are usually observed to increase from cloud top toward base [McFarquhar and Heymsfield, 1998; Heymsfield *et al.*, 2006]. Several mechanisms may contribute to such structure. Ice particle size and growth rate are strongly dependent on ambient humidity and temperature. In situ measurements are indicative of the decreases of water vapor available for ice particle growth as the temperature decreases toward cloud top. As they fall from cloud top, ice particles usually grow in size. The warmer and more humid conditions below cloud top are certainly important, but the collision-coalescence processes may also play a role [Pruppacher and Klett, 1997]. The fact that larger ice particles generally fall faster operates as a size-sorting mechanism that leads to the increasing toward base size profile [Heymsfield *et al.*, 2002].

[5] The vertical inhomogeneity of cloud particle size is known to have significant effects on the r_e and IWP retrievals based on the SRBS method. Several studies [e.g., Nakajima and King, 1990; Han *et al.*, 1994] showed that the SRBS method applied assuming vertical homogeneity of the cloud properties, tends to overestimate the liquid water path of water clouds. The retrieved r_e generally corresponds to the r_e of the cloud layer at about 20–40% of the total optical depth of the cloud depending on the vertical profile of cloud droplet size [Nakajima and King, 1990]. In a study of photon transport in vertically inhomogeneous water clouds, Platnick [2000] introduced the concept of a reflectance weighting function to quantify the relation between the SRBS retrieved r_e on the basis of a homogenous cloud assumption and the actual vertical profile of r_e . As expected, it was found that retrievals based on different SWIR wavelengths are sensitive to different parts of the water clouds. For example, the r_e retrieval using the 3.7 μm band is sensitive to the uppermost portion of the cloud, while the 1.6 and 2.1 μm bands penetrate deeper into the cloud, though the relative relationship depends significantly on the vertical structure and the solar/viewing geometry. The effects of vertical cloud particle size inhomogeneity on the SRBS method were also discussed from different perspectives in several other studies [e.g., Han *et al.*, 1994; Platnick

et al., 2000; *Chang and Li*, 2002; *Kokhanovsky*, 2004; *Rozanov and Kokhanovsky*, 2005] and similar findings were reported. It is worth mentioning that recently substantial attempts have been made to incorporate the cloud vertical structure in the SRBS algorithm [e.g., *Brenguier et al.*, 2000; *Chang and Li*, 2002, 2003; *Schuller et al.*, 2003; *Bennartz*, 2007; *Wang et al.*, 2009].

[6] While vertical inhomogeneity effects on the SRBS method have been relatively well studied for liquid water clouds, less is known about the effect on ice cloud retrievals, in part, owing to the difficulty in constraining realistic vertical microphysical structures from in situ observations or models. This is, however, an important issue for a number of reasons. To be more specific, it is important to know to what extent ice cloud properties retrieved from either method are representative of column means. For a given vertically inhomogeneous ice cloud, does the IRSpW method tend to underestimate or overestimate IWP, and why? Furthermore, if the cloud vertical inhomogeneity affects the SRBS and the IRSpW method differently, what is the significance of the discrepancy? Does the discrepancy of the two methods provide useful information about the vertical structure of ice clouds? These questions must be addressed before comparing or combining ice cloud retrievals from the SRBS and IRSpW methods. Answers to these questions may provide guidance for the use of satellite-based ice cloud retrievals in, for example, validation of GCMs, aerosol indirect studies, and parameterization development.

[7] To seek answers to the above questions, we investigate the effects of ice particle size vertical inhomogeneity on cloud retrievals. In contrast to the previous studies, we will assess the effects on both the SRBS and IRSpW with an emphasis on understanding the consistency between the two under different inhomogeneous ice cloud conditions. The paper is organized as follows: The ice particle microphysical and optical model used in this study is introduced in section 2. The inhomogeneity effects on the SRBS method are discussed in section 3.1, with a revisit to the concept of the reflectance weighting function. In section 3.2, we will elucidate how vertical inhomogeneities affect the IRSpW method. In section 4 the major findings will be summarized and some implications discussed.

[8] Unless stated otherwise, in the rest of this paper we denote the visible optical thickness of the entire ice cloud layer as τ_c , the visible optical depth from cloud top to some level within the clouds as τ , and the vertical profile of effective radius as $r_e(\tau)$. We denote the retrievals based on the homogeneous cloud assumption as τ_c^* , r_e^* and IWP^* .

2. Ice Cloud Bulk Scattering Model and Radiative Transfer Model

[9] The ice cloud bulk scattering models used in this study are the same as those used in the MODIS Collection 5 (MOD06) algorithm [*Baum et al.*, 2005a, 2005b] (hereafter this model is referred to as “Baum05 model”). In this model, ice particles are categorized into six habits, including droxtal [*Zhang et al.*, 2004], hexagonal columns and plates, hollow columns, bullet rosettes and aggregates [*Yang et al.*, 2000]. The variation of habit with the ice particle size (D) is

described with a size-dependent habit distribution. Following [*Foot*, 1988; *Francis et al.*, 1994], the effective radius of ice particles are defined to be consistent with the definition for water droplets; that is,

$$r_e = \frac{3 \sum_i \int_0^\infty V_i(D) f_i n(D) dD}{4 \sum_i \int_0^\infty A_i(D) f_i n(D) dD}, \quad (1)$$

where subscript i indicates ice crystal habit; f_i indicates the weight of the i th habit; and A are the volume and projected area of ice particles, respectively, and $n(D)$ is the ice particle size distribution (PSD). More than 1000 in situ measured PSDs are used to derive the mean, as well as the variation, of the ice particle bulk scattering properties.

[10] The radiative transfer computations involved in this study are carried out using the DISORT model developed by [*Stamnes et al.*, 1988]. The adjoint method [*Marchuk*, 1964; *Box et al.*, 1988; *Box*, 2002] is applied to DISORT to compute the weighting functions that are needed in later sections.

3. Retrieval Methods

[11] Section 3.1 gives a brief overview of the SRBS and IRSpW methods. Both methods are well established. Their theoretical basis, strengths and limitations are well documented in the literature. Here, we only revisit the more relevant aspects of the two methods.

3.1. Solar Reflectance Bispectral Method

[12] In the SRBS method, τ_c^* and r_e^* are simultaneously retrieved from a pair of satellite-observed cloud bidirectional reflectances, each with different amounts of bulk water absorption [*Nakajima and King*, 1990]. Because ice absorption in the VIS/NIR spectral region, for example at $0.8 \mu\text{m}$, is negligible, the single scattering albedo (ω) of ice particles is essentially unity for all r_e (Figure 1a). As a result, cloud reflectance, $R(0.8 \mu\text{m})$, is a strong function of τ_c , and only weakly dependent on r_e (and then only via sensitivity to the phase function). In the SWIR spectral region, for example at $2.1 \mu\text{m}$, the stronger ice absorption makes ω and consequently $R(2.1 \mu\text{m})$ quite sensitive to the r_e . A sensitivity study by *Yang et al.* [2001] shows that the bidirectional reflectance at the top of the atmosphere (TOA) at a visible wavelength (say, $0.65 \mu\text{m}$) is not sensitive to the vertical structure (i.e., particle habit and size profile) of an ice cloud whereas a strong sensitivity is noticed for a near-infrared wavelength.

[13] A combination of $R(0.8 \mu\text{m})$ and $R(2.1 \mu\text{m})$ provides two pieces of information attributed to τ_c^* and r_e^* . In practice, τ_c^* and r_e^* are retrieved by mapping satellite observations onto the so-called look-up tables (LUT) that contain precomputed $R(0.8 \mu\text{m})$ and $R(2.1 \mu\text{m})$ under various conditions. An example of such a LUT is shown in Figure 1b. It should be pointed out that other combinations of wavelengths are also frequently used in the SRBS method. For example, in addition to the baseline r_e^* retrieval at $2.1 \mu\text{m}$ (i.e., $r_e^*(2.1 \mu\text{m})$), the r_e^* values based on the 1.6 and $3.7 \mu\text{m}$ observations are also reported in the MODIS cloud product [*Platnick et al.*, 2003].

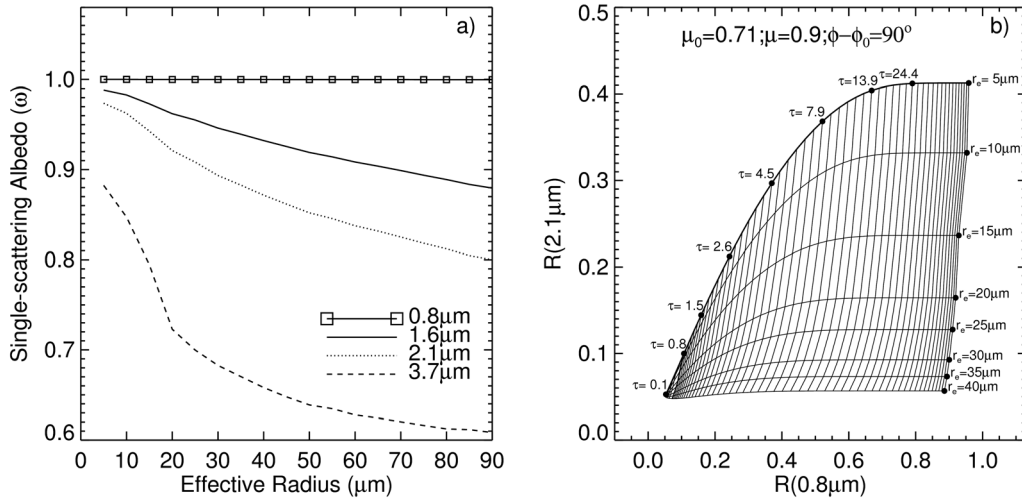


Figure 1. (a) Single-scattering albedo (ω) of ice particles at different VIS and NIR wavelengths as a function of ice particle effective radius (r_e). (b) An example of the LUT for the SRBS method.

3.2. IR Split-Window Method

[14] The IRSpW method utilizes a pair of radiance observations in the infrared (IR) atmospheric window region, from about 8 μm to 13 μm , for ice cloud τ_c^* and r_e^* retrieval [Inoue, 1985, 1987; Prabhakara *et al.*, 1988]. Because ice particles have strong absorption in this spectral region [Warren, 1984], ice clouds can significantly block the radiation from the warm surface and re-emit at a much lower temperature. Therefore, for an IR satellite sensor outside of polar inversions, an ice cloudy pixel appears colder than the surface temperature and the thicker the cloud the colder the pixel's brightness temperature. If the properties (i.e., temperature and emissivity) of the underlying surface and cloud top position are known, τ_c^* can be inferred from the difference between the upwelling radiance at cloud base and the satellite-observed radiance. Figure 2a shows the absorption efficiency (Q_a) of ice particles at three IR wavelengths, 8.5, 11, and 12 μm . Generally, at the same r_e , $Q_a(8.5\mu\text{m}) < Q_a(11\mu\text{m}) < Q_a(12\mu\text{m})$. For this reason, the

same ice cloud absorbs more surface emission and therefore appears colder, for example, at 12 μm than at 8.5 μm . Figure 2b shows the differences of Q_a between the three wavelengths as functions of r_e . The strong dependence of Q_a difference (for example, $Q_a(8.5\mu\text{m}) - Q_a(12\mu\text{m})$) on r_e makes it possible to infer r_e from the difference between observations at two different bands.

[15] Since absolute radiances at difference wavelengths are not directly meaningful, in the retrieval they are usually converted to other metrics, such as the brightness temperature (BT). However, the conversion from radiance to BT is highly nonlinear. To derive weighting functions for the IRSpW method later in this study, we use a more physically meaningful metric, the apparent emissivity ε_{ap} , defined as:

$$\varepsilon_{ap}(\lambda) = I_{obs}(\lambda) / B(\lambda, T_c), \quad (2)$$

where I_{obs} is the satellite-observed radiance at the wavelength λ . $B(\lambda, T_c)$ denotes the Planck function at the radiative cloud top temperature T_c . Note that the dependence of

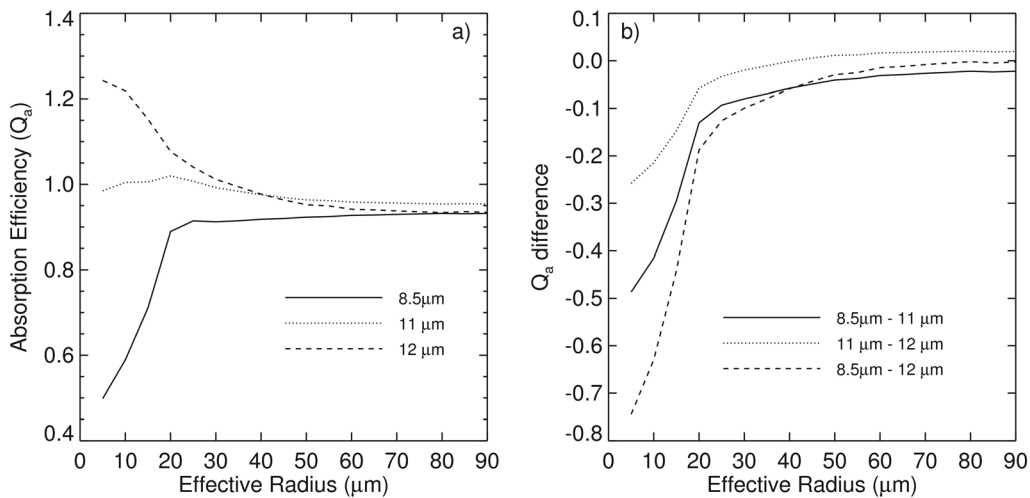


Figure 2. (a) Absorption efficiency (Q_a) of ice particles at 8.5, 11, and 12 μm as a function of r_e . (b) Difference of Q_a between difference wavelengths as a function of r_e .

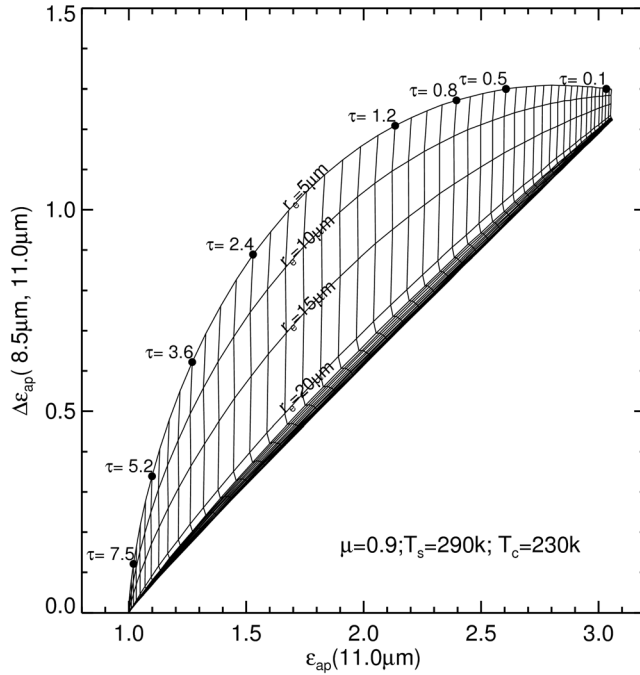


Figure 3. An example of the LUT for IRSpW method. The x axis is the satellite-observed apparent emissivity ε_{ap} (see equation (2) for the definition) at $11 \mu\text{m}$, and the y axis is the difference of ε_{ap} between 11 and $12 \mu\text{m}$.

ε_{ap} on cloud and surface properties, and the satellite viewing geometry, has been omitted in equation (2) for simplicity. The τ_c^* and r_e^* are retrieved using the precomputed look-up tables, with one dimension being ε_{ap} (for example $\varepsilon_{ap}(11\mu\text{m})$ and the other the difference in ε_{ap} between two wavelengths (for example $\varepsilon_{ap}(8.5\mu\text{m}) - \varepsilon_{ap}(11\mu\text{m})$). An example of such look-up table is shown in Figure 3. It should be clarified that there is no fundamental difference between using ε_{ap} or BT for the split-window method. The ε_{ap} is nevertheless used in this study because, as will be shown later, its simplicity facilitates a straightforward weighting analysis to illustrate the effects of vertical inhomogeneity on the split-window method. It should also be pointed out that for the sake of simplicity we assume homogenous cloud temperature throughout this study. In practice, T_c can be obtained from cloud top property techniques, for example the CO_2 -slicing method. We note that so-called beta ratios [Parol et al., 1991; Heidinger and Pavolonis, 2009] provide a useful microphysical mapping for radiance differences from homogeneous clouds, but were not conducive to the weighting analysis adopted later.

4. Effects of Cloud Vertical Inhomogeneity on Cloud Property Retrieval

[16] When applying the above-described SRBS and IRSpW methods to a vertically inhomogeneous ice cloud, the retrieval algorithm seeks a homogenous ice cloud that has the same radiative effect; for example, observed $R(0.8\mu\text{m})$ and $R(2.1\mu\text{m})$. Such retrievals give rise to several questions. For example, how does the size retrieval vary with the vertical structure of the cloud? If error is defined in

terms of the inferred IWP (proportional to product of effective radius and cloud layer optical thickness), how does the IWP error depend on the spectral method used for the retrieval? Is it possible that the cloud vertical inhomogeneity affects the SRBS and the IRSpW methods in quite different ways leading to disparate retrievals?

[17] The key to answering the above questions, which is the focus of this section, is to understand the underlying physics that drives the sensitivity of the retrieved effective radius to the vertical structure of the effective radius profile through the cloud. To make the discussion easier, we discuss optically thin ($\tau_c \leq 1$) and moderately thick ($1 < \tau_c \leq 5$) clouds separately. As will be discussed momentarily, when the cloud is thin, the radiative transfer process is relatively simple, and the sensitivity to the homogenous cloud assumption can be understood as the result of the nonlinear dependence of ice particle scattering properties on effective radius. When the cloud is moderately thick, the radiative transfer process becomes more complicated and a more involved weighting analysis is needed to understand r_e^* retrievals. It should be noted that there is no clear separation of “thin” from “moderately thick” clouds. The transition is continuous rather than discrete. Therefore, the optical thickness regions used here only provide a qualitative basis for the discussion. Thick ice clouds ($\tau_c > 5$) are not included in the discussion below for a couple of reasons. The first is that, as one can observe from Figure 3, when cloud τ_c becomes thicker than about 5, the LUT for IRSpW method begins to lose its orthogonality, which makes the retrieval results more subject to numerical errors than cloud vertical inhomogeneity. The other is the difficulty to make quantitative assessment of the IRSpW retrieval results using some simple scheme (see section 4.2.2 for details).

4.1. Thin Ice Clouds ($\tau_c \leq 1$)

[18] The radiative transfer process in optically thin clouds is relatively simple. As pointed out by [Marshak et al., 2006], the effect of cloud inhomogeneity is attributed mainly to the nonlinear dependence of ice particle scattering properties on ice particle size (as opposed to nonlinear radiative effects due to multiple scattering).

[19] To illustrate this effect in the case for SRBS, let us consider the following case: an optically thin ice cloud layer with an optical thickness of $\Delta\tau_c$ and an effective radius of $r_{e,1}$ overlies another layer with the same $\Delta\tau_c$ but a different effective radius $r_{e,2}$. On the basis of the adding principle [Chandrasekhar, 1960], it can be shown that, for small $\Delta\tau_c$, the reflectance of the combined layer is

$$R_{12}(\lambda) = R(\lambda, r_{e,1}) + R(\lambda, r_{e,2}) + \delta(\Delta\tau_c^2), \quad (3)$$

where $R(\lambda, r_{e,1})$ and $R(\lambda, r_{e,2})$ are the reflectances of the upper and lower layers, respectively. The term, $\delta(\Delta\tau_c^2)$, contains higher-order scattering terms. It is well known that when a cloud is infinitesimally thin, its reflectance is proportional to:

$$R(\lambda, r_e) \approx C_1 \omega(\lambda, r_e) P(\lambda, r_e) \Delta\tau_c, \quad (4)$$

where C_1 is a constant, P is the scattering phase function. At VIS/NIR wavelengths, such as $0.8 \mu\text{m}$, neither ω (single scattering albedo) nor P depends strongly on r_e . As a result,

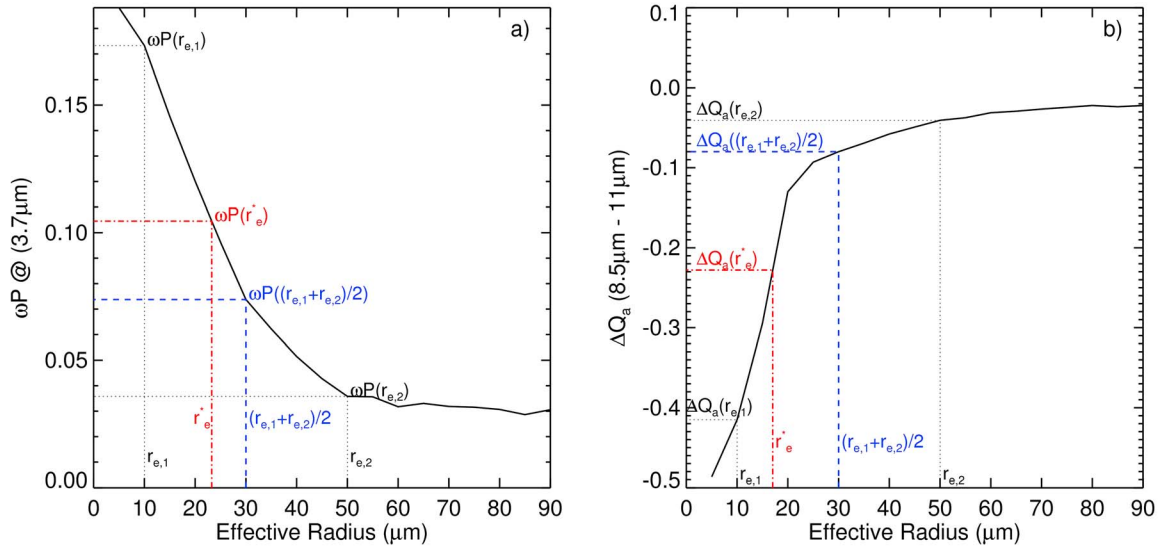


Figure 4. Illustration of the nonlinearity effect on averaging. (a) An example for the SRBS method. (b) An example for the IRSpW method. See section XX for further details.

the retrieved $\Delta\tau_c^*$ from R_{12} can be expected to be close to $2\Delta\tau_c$. As for the effective radius retrieval, the process is essentially to find a r_e^* that satisfies $\omega(r_e^*)P(r_e^*) = [\omega(r_{e,1})P(r_{e,1}) + \omega(r_{e,2})P(r_{e,2})] / 2$ for the NIR wavelength. As shown in Figure 4a, ωP at $3.7\mu\text{m}$ and a scattering angle of 140° is nonlinearly dependent on r_e . Consequently, the retrieved r_e^* is smaller than the linear average of $r_{e,1}$ and $r_{e,2}$ (i.e., $r_e^* < (r_{e,1} + r_{e,2}) / 2$) which is needed for an unbiased IWP retrieval. The nonlinearity effect on cloud property retrievals has been well studied in the literature [e.g., Oreopoulos and Davies, 1998; Marshak et al., 2006].

[20] The nonlinearity effect is also inherent in the IRSpW method. It can be shown that the difference in apparent emissivity between two bands (i.e., $\Delta\varepsilon_{ap}$) for the combined layer in the above example is approximately:

$$\Delta\varepsilon_{ap} \approx C_2 [\Delta Q_a(r_{e,1}) + \Delta Q_a(r_{e,2})]. \quad (5)$$

Therefore, the retrieval is essentially to find a r_e^* that satisfies $\Delta Q_a(r_e^*) = [\Delta Q_a(r_{e,1}) + \Delta Q_a(r_{e,2})] / 2$. Once again, the highly nonlinear dependence of ΔQ_a on r_e may lead to r_e^* retrievals that are substantially smaller than $(r_{e,1} + r_{e,2}) / 2$.

[21] Interestingly, as one can see by comparing retrieval results in Figures 4a and 4b, the nonlinearity effect is stronger for the IRSpW method than for the SRBS method. Offline analyses (not shown here) indicate that the nonlinearity effect of other combinations of IR bands is somewhat similar to the combination of 8.5 and $11\mu\text{m}$ shown in Figure 4b, and the effect associated with the retrieval using the $1.6\mu\text{m}$ or $2.1\mu\text{m}$ bands is weaker than that of $3.7\mu\text{m}$ shown in Figure 4a. Therefore, the difference in the magnitude of the nonlinearity effect between SRBS and IRSpW depends on channel selection. The physical reason for this difference is not well understood. It may be a result of different behaviors of ice particle scattering properties in IR and SWIR spectral regions [van de Hulst, 1957; Yang et al., 2000, Yang et al., 2005]. The use of artificial particle size distributions for the computation of the bulk scattering properties of small ice particles in the work of [Baum et al.,

2005a, 2005b] might also play a role here, although the use of realistic size distributions would seem more likely to change the order of nonlinearity, than lead to a perfect match, between different bands. Regardless of the reasons, an important implication of this difference in the magnitude of nonlinearity effect is that, if an ice cloud is optically thin with substantial ice particle size variation from cloud top to base, the r_e^* retrievals based on the SRBS and the IRSpW for the same cloud may be quite different.

[22] To conclude, when an ice cloud is optically thin, the cloud vertical inhomogeneity manifests itself in the effective radius retrieval as the nonlinearity effect of scattering properties versus effective radius. Owing to this effect, the retrieved r_e^* is weighted more toward the small ice particles, leading to an underestimation of IWP in both the SRBS and IRSpW methods. Generally, the nonlinearity effect is stronger in the IRSpW method than in the SRBS method, potentially causing a significant discrepancy between the two retrieval methods.

4.2. Moderately Thick Ice Clouds ($1 < \tau_c \leq 5$)

[23] As the cloud becomes optically thicker, the radiative transfer process becomes more complicated. To understand the underlying physics that controls the errors caused by the homogenous cloud assumption in this regime, the following two inhomogeneous ice cloud cases are studied. In case A, r_e is assumed to increase linearly with the visible optical thickness from $15\mu\text{m}$ at cloud top to $45\mu\text{m}$ at cloud base. Case B is the reverse, with r_e decreasing linearly with τ from $45\mu\text{m}$ at cloud top to $15\mu\text{m}$ at cloud base. The total visible optical thickness of the cloud is assumed to be 3.0 in both cases. For the SRBS method, the surface is assumed to be dark (i.e., zero reflectance). For the IRSpW method, the cloud is assumed to have a homogeneous temperature of 230 K ; the surface emissivity is assumed to be 0.97 for all wavelengths and the surface temperature is set to 290 K (corresponding to a surface brightness temperature of 297 K). Atmospheric absorption is not considered. While these two cases are rather simple and may not represent

Table 1. Retrieved τ_c^* , r_e^* and the IWP Derived From 2/3 $\rho_{ice}\tau_c^*r_e^*$ on the Basis of the SRBS and IRSpW Method for Cases A and B^a

λ (μm)	τ_c^*	r_e^* Retrieval (μm)	r_e^* Estimate (μm)	IWP Retrieval (g/m^2)
<i>Case A^b</i>				
0.86 and 1.6	2.87	25.81	26.56	44.44
0.86 and 2.1	2.85	25.40	25.47	43.43
0.86 and 3.7	2.66	20.73	22.10	33.04
11 and 12	3.16	24.39	24.10	46.24
8.5 and 11	3.06	23.61	22.10	43.34
8.5 and 12	3.06	24.00	22.65	44.06
<i>Case B^c</i>				
0.86 and 1.6	3.07	30.64	31.60	56.43
0.86 and 2.1	3.08	30.96	31.28	57.21
0.86 and 3.7	3.28	34.78	33.81	70.53
11 and 12	3.15	24.57	24.10	46.43
8.5 and 11	2.99	20.26	22.10	36.34
8.5 and 12	2.97	22.46	22.65	40.02

^aThe r_e^* estimated from the weighting function are also listed. Italicized entries correspond to the IRSpW method, while the nonitalicized values correspond to the SRBS method.

^bWhere $\tau_c = 3.0$; cloud top, $r_e(0) = 15\mu\text{m}$, cloud base $r_e(\tau_c) = 45\mu\text{m}$; and IWP = 54 (g/m^2).

^cWhere $\tau_c = 3.0$; cloud top, $r_e(0) = 45\mu\text{m}$, cloud base $r_e(\tau_c) = 15\mu\text{m}$; and IWP = 54 (g/m^2).

typical ice clouds, the intent here is to study the underlying physics. Retrievals based on observed ice cloud profiles will be studied later in section 4.3.

4.2.1. Effects on the Solar Bispectral Method

[24] The retrievals based on the SRBS method for the above two cases are shown in Table 1. Evidently, the vertical variation of ice particle size strongly affects the SRBS retrieval results. In case A, when r_e increases from cloud top toward base, the SRBS method tends to slightly underestimate τ_c . The r_e^* retrievals are all significantly smaller than 30 μm , the linear average of r_e over the entire cloud layer. Consequently, the derived IWPs are all significantly smaller than the true values. When the 3.7 μm is used in the retrieval, the IWP is underestimated by as large as about 40%. It needs to be pointed out that the observed daytime radiance at 3.7 μm includes the contributions from both solar reflection and thermal emission by the ice clouds. To resolve the reflected signals and infer r_e , the thermal emission component has to be accounted for utilizing the information in thermal emission channels. The accuracy of this step is critical to the retrieval of low and warm water clouds, while less important for ice clouds. This is because for warm water clouds the thermal emission can typically contribute about half of the observed 3.7 μm radiance [Platnick and Valero, 1995], while for cold ice clouds the contribution is only about 2–5% [Sherwood, 2002]. In this study, we assume that the thermal emission component has been perfectly removed from the 3.7 μm observation, by omitting the thermal emission in both forward radiative transfer simulation and retrieval. In case B, when r_e decreases from cloud top toward base, the SRBS method tends to slightly overestimate τ_c . The IWPs based on $r_e^*(1.6\mu\text{m})$ and $r_e^*(2.2\mu\text{m})$ in this case are close to the true value, while IWP based on the 3.7 μm retrieval is more than 30% larger.

[25] The SRBS retrieval results can be easily understood utilizing the concept of weighting function [Platnick, 2000]. In that study, it was demonstrated for water clouds that r_e^*

retrieved from the SRBS method can be approximately related to the effective radius profile $r_e(\tau)$ through a weighted integral:

$$r_e^*(\lambda) = \int_0^{\tau_c} r_e(\tau) w(\lambda, \tau) d\tau, \quad (6)$$

where $w(\lambda, \tau)$ is the normalized weighting function. One of the two successful weighting functions explored in that study is based on the maximum penetration of reflected photons:

$$w_m(\lambda, \tau, \tau_c) = \frac{1}{R(\lambda, \tau_c)} \frac{dR(\lambda, \tau)}{d\tau}, \quad (7)$$

where $R(\tau_c)$ is reflectance of the entire cloud layer and $R(\tau)$ is the reflectance from the cloudy portion above the level τ . The weighting function in equation (7) is defined to represent the sensitivity of the satellite-observed cloud reflectance to each level in the cloud. It is a quantitative description of the understanding that if the observed reflectance is more sensitive to the upper than the lower portion of the cloud, the retrieved r_e^* should be closer to the r_e of the upper levels.

[26] The weighting functions for the above two cases are shown in Figure 5. Some interesting observations can be made. First of all, the weighting functions for the SRBS method, in both cases and for all wavelengths, are weighted more toward the cloud top as expected. This feature explains clearly why in case A (B) the retrieved r_e^* is smaller (larger) than 30 μm (i.e., the r_e at cloud center) and why the IWP is underestimated (overestimated). Second, it is evident that $w_m(3.7\mu\text{m})$ is weighted closer toward cloud top than $w_m(1.6\mu\text{m})$ and $w_m(2.1\mu\text{m})$. As a result, $r_e^*(3.7\mu\text{m})$ is about 5 μm smaller (larger) than $r_e^*(1.6\mu\text{m})$ and $r_e^*(2.1\mu\text{m})$ in case A (B). It is also interesting to note that $w_m(1.6\mu\text{m})$ and $w_m(2.1\mu\text{m})$ for case A (Figure 5a) are weighted more toward cloud top than their counterparts in case B (Figure 5b). Such differences are expected as the more reflective small ice particles (Figure 1a) overlie less reflective large particles in case A, as opposed to the reverse in case B. The r_e^* estimated from the weighting functions based on equation (6) are also listed in Table 1. As suggested by the close agreement (within 1 μm) between the estimations and the actual retrievals, the weighting function of equation (7) not only qualitatively captures the physics underlying the SRBS method, but also quantitatively predicts the r_e^* retrieval with reasonable accuracy.

4.2.2. Effects on the IR Split-Window Method

[27] The τ_c^* and r_e^* retrievals for the two cases using the IRSpW method (with a homogenous cloud assumption) and different wavelength combinations are listed in Table 1. Several points are worth noting in the table. First, the retrieval differences between cases A and B are smaller than for the SRBS method. Indeed, the τ_c^* and r_e^* retrievals in both cases are almost the same when the 11 μm and 12 μm combination is used. Second, the r_e retrievals in both cases are smaller than 30 μm and consequently IWP retrievals are substantially smaller than the true value. Previous studies have noticed similar behavior of the IRSpW method. For example, Chung et al. [2000] found that the high-spectral resolution cloud forcing of ice clouds in the infrared is

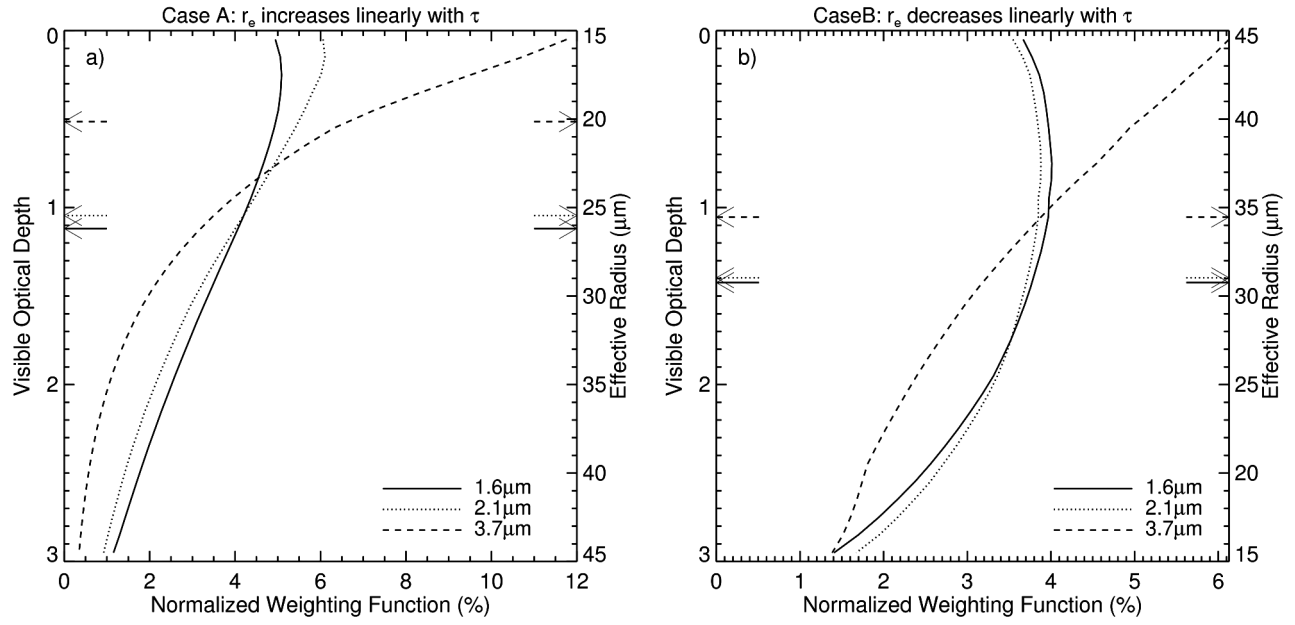


Figure 5. The normalized weighting functions for the r_e^* retrieval in the SRBS method for (a) case A and (b) case B.

relatively insensitive to cloud vertical structure and weighted toward smaller ice particle size. However, the reason for such behavior is not given. In the following part of this section, we elucidate the underlying physics that determines the sensitivity of the IRSpW method to the vertical variation in ice particle size.

[28] In light of the success of weighting function in the SRBS method, we also developed two sets of weighting functions, $w_\varepsilon(\lambda, \tau)$ and $w_{\Delta\varepsilon}(\lambda_1, \lambda_2, \tau)$, to help understand the retrieval results from the IRSpW method. A brief derivation

for these weighting functions is given in Appendix A. The weighting function w_ε represents the sensitivity of the observed $\varepsilon_{ap}(\lambda)$ to each level in the cloud, as well as the surface. Similarly, $w_{\Delta\varepsilon}$ represents the sensitivity of $\varepsilon_{ap}(\lambda_1, \tau) - \varepsilon_{ap}(\lambda_2, \tau)$ to each sublayer of the cloud and the surface.

[29] Figure 6 shows the normalized w_ε as a function of visible optical depth for the three wavelengths 8.5, 11, and 12 μm for cases A and B. Because the weighting contribution for the surface is much larger than that for cloud, they

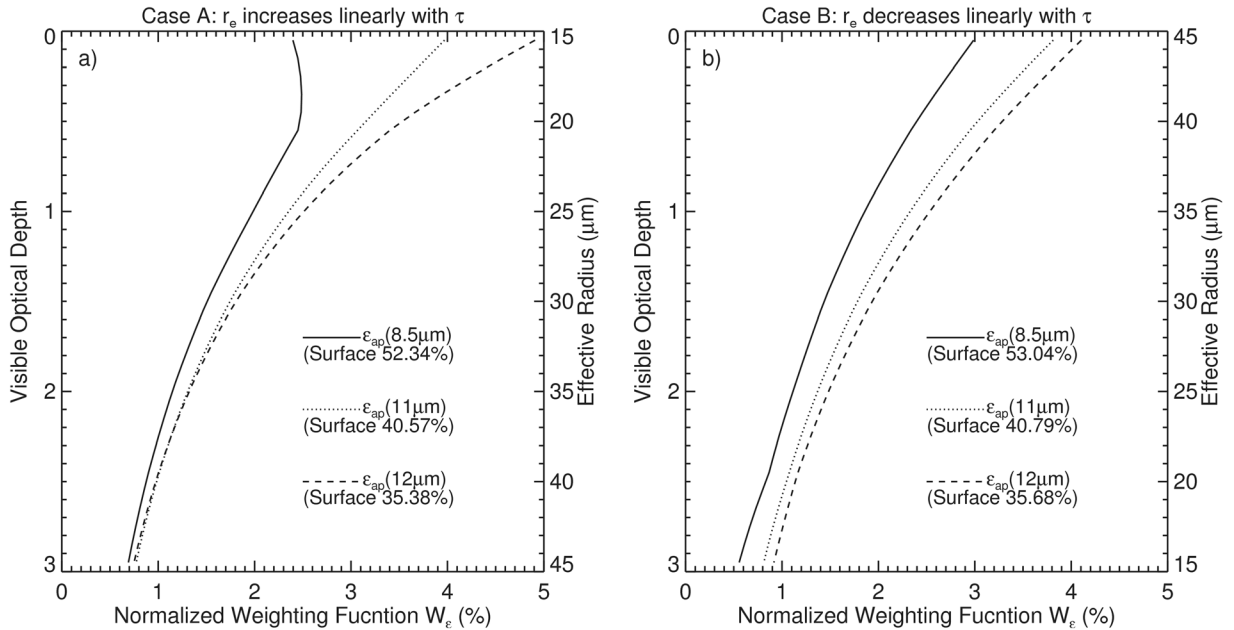


Figure 6. The normalized weighting functions for ε_{ap} for (a) case A and (b) case B.

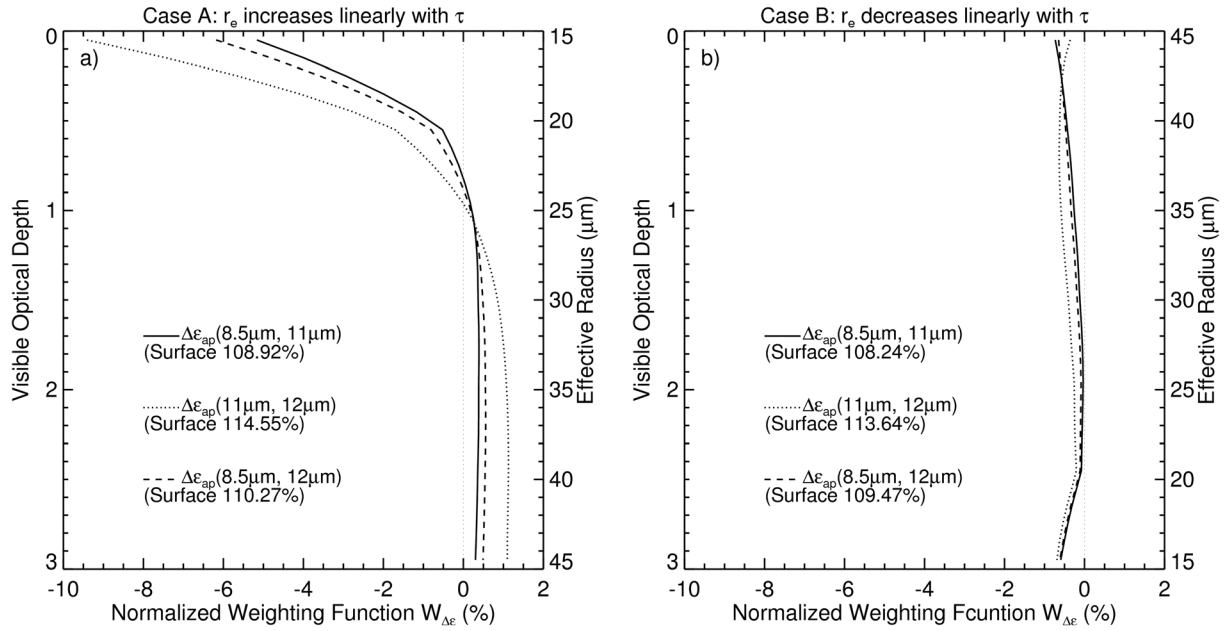


Figure 7. The normalized weighting functions for $\Delta\epsilon_{ap}$ for (a) case A and (b) case B.

are not plotted in Figure 6 for the sake of clarity, but the values are given. From the values of w_ϵ for the surface, it can be estimated that the whole cloud contributes from about 50% to 65% of the observed ϵ_{ap} , depending on the wavelength. These numbers indicate that when the cloud is moderately thick ($\tau_c = 3$ in the example), the transmission of surface radiation and cloud emission are almost equally important for the observed ϵ_{ap} . An implication is that an accurate specification of cloud emission is important for the τ_c^* retrieval using the IRSpW method. Indeed, this point has been discussed in many studies. For instance, *Cooper et al.* [2003] showed that uncertainties in the τ_c^* can be greatly reduced if explicit cloud boundary information from spaceborne lidar and radar is used in the IRSpW method to specify the cloud emission.

[30] Figure 7 shows the weighting function $w_{\Delta\epsilon}$ for both cases. Once again, $w_{\Delta\epsilon}$ represents the sensitivity of $\Delta\epsilon_{ap}(\tau, \lambda_1, \lambda_2)$ to each cloud level (should not be confused with the r_e retrieval weighting function in equation (7)). To understand Figure 7, one must keep in mind that $\Delta\epsilon_{ap}$ is determined by two opposite and competing processes that tend to cancel each other. Take the combination of 8.5 and 11 μm for example. As shown in Appendix A, the weighting function $w_{\Delta\epsilon}(8.5 \mu\text{m}, 11 \mu\text{m}, \tau)$ can be decomposed as $Q_a(8.5 \mu\text{m}, \tau)E(8.5 \mu\text{m}, \tau) - Q_a(11 \mu\text{m}, \tau)E(11 \mu\text{m}, \tau)$. The term Q_a denotes the absorption (and thus emission) efficiency of ice particles. The term $E(\lambda, \tau)$ denotes the so-called escape function. Its physical interpretation is the amount of radiation at the wavelength λ that escapes to cloud top from a unit emission source located at an optical depth level τ in the cloud. Because of the weak scattering in the thermal infrared spectral region, E is largely determined by the absorption of the cloud portion above τ ; that is, $E \sim e^{-\tau_a}$. The sign and magnitude of $w_{\Delta\epsilon}$ are determined by the competition between two opposite processes; that is, layer emission versus layer absorption of upwelling radiation. The

predominance of the former tends to lead to negative $w_{\Delta\epsilon}(8.5 \mu\text{m}, 11 \mu\text{m}, \tau)$ because generally $Q_a(8.5 \mu\text{m}) < Q_a(11 \mu\text{m})$, whereas the predominance of the latter leads to positive $w_{\Delta\epsilon}(8.5 \mu\text{m}, 11 \mu\text{m}, \tau)$ because generally $E(8.5 \mu\text{m}, \tau) > E(11 \mu\text{m}, \tau)$ (see Figure 2). Bearing this in mind, we return to Figure 7.

[31] In case A, ice particle size is small at cloud top and increases toward cloud base. At cloud top, both $E(8.5 \mu\text{m}, \tau)$ and $E(11 \mu\text{m}, \tau)$ are close to unity, but the $Q_a(8.5 \mu\text{m})$ of small ice particles is substantially smaller than their $Q_a(11 \mu\text{m})$. For these reasons, a relatively large negative $w_{\Delta\epsilon}$ is observed at cloud top in this case (Figure 7a). As r_e increases toward cloud base, the difference between $Q_a(8.5 \mu\text{m})$ and $Q_a(11 \mu\text{m})$ decreases (Figure 2b), leading to a decrease in the emission effect. On the other hand, the absorption efficiency at 8.5 μm increases with increasing optical depth. The compensation of the two effects results in $w_{\Delta\epsilon}$ changing sign inside the cloud at the $\tau \approx 1$ level. For the part of the cloud above this level, the emission effect dominates the net contribution from $\Delta\epsilon_{ap}(8.5 \mu\text{m}, 11 \mu\text{m})$, and for the part below, the absorption effect dominates. Overall, the entire cloud has a small negative impact on the observed $\Delta\epsilon_{ap}(8.5 \mu\text{m}, 11 \mu\text{m})$, indicating the weak predominance of the emission effect. For case B in Figure 7b, because large ice particles are at cloud top and for large ice particles the difference between $Q_a(8.5 \mu\text{m})$ and $Q_a(11 \mu\text{m})$ is small (see Figure 2), the magnitude of $w_{\Delta\epsilon}$ at cloud top in case B is substantially smaller than that in case A. Unlike in case A, $w_{\Delta\epsilon}$ for case B remains negative, albeit small, throughout the whole cloud, indicating the weak predominance of the emission effect in this case.

[32] The spectral variance of surface emissivity in the thermal IR is generally small for vegetation and water surfaces [*Masuda et al.*, 1988]. As mentioned at the beginning of section 4.2, we have assumed a constant surface emissivity for all wavelengths. Therefore, in both our cases, the

contribution of the surface to $\Delta\varepsilon_{ap}$ is completely determined by the effect of the cloud spectral absorption on surface emission that is transmitted through the entire ice cloud layer. Because of this, as well as the aforementioned cancellation mechanism that regulates the cloud's contribution, $w_{\Delta\varepsilon}$ for the surface is positive and much larger than that of the cloud.

[33] It is clear from the preceding analyses that the signal for the r_e^* retrieval in the IRSpW method (i.e., $\Delta\varepsilon_{ap}$) comes predominately from the surface for the two cases considered. This is in contrast to τ_c^* which is essentially derived from $\varepsilon_{ap}(11\ \mu\text{m})$ observations (Figure 3). As shown in Figure 6, $\varepsilon_{ap}(11\ \mu\text{m})$ is similarly impacted by the surface and the cloud contributions. This difference is probably the reason why Cooper *et al.* [2003] noticed that explicit cloud boundary information has only small impact on r_e^* retrieval based on the IRSpW method. The predominance of the surface contribution to $\Delta\varepsilon_{ap}$ also explains why the r_e^* retrievals in cases A and B are quite similar. It is because in the thermal IR ice particle scattering is weak and the absorption process dominates the radiative transfer from surface to cloud top. The absorption part of the cloud transmittance depends on the total τ_a of the cloud, but not on the detailed vertical profile of absorption (r_e).

[34] Having obtained an understanding of the physics underlying the IRSpW method, we are now in the position to make a quantitative estimate of the r_e^* retrieval for a given inhomogeneous ice cloud. The difficulty in following the approach of Plattnick [2000] directly for retrievals involving emission (which were investigated for water clouds that were optically thick in the emissive channels; see Plattnick [2000]) is the potentially significant surface contribution for ice clouds requiring an appropriate value of r_e to be assigned to the surface to close the integral. On the flip side, however, the predominance of a surface contribution to $\Delta\varepsilon_{ap}$ suggests that whatever value of r_e is assigned to the surface, it will be fairly close to r_e^* . Therefore, it seems that a reasonable way to estimate the r_e^* retrieval for a moderately transparent inhomogeneous cloud is to ignore the small contributions from the cloud, as well as the weak cloud scattering, and focus only on the absorption of surface emission by the cloud. As such, r_e^* can be approximated by the following equation:

$$\begin{aligned} \varepsilon_s(\lambda_1)B(\lambda_1 T_s)e^{-\tau_a(\lambda_1, r_e(\tau))} - \varepsilon_s(\lambda_2)B(\lambda_2 T_s)e^{-\tau_a(\lambda_2, r_e(\tau))} = \\ \varepsilon_s(\lambda_1)B(\lambda_1 T_s)e^{-\tau(\lambda_1, r_e^*)} - \varepsilon_s(\lambda_2)B(\lambda_2 T_s)e^{-\tau(\lambda_2, r_e^*)} \end{aligned} \quad (8)$$

where $\tau_a(\lambda, r_e(\tau))$ and denote $\tau_a(\lambda, r_e^*)$ the actual and estimated absorption optical thickness of the ice cloud. The r_e^* retrievals estimated from equation (8) are given in Table 1. Note that the estimated r_e^* for case A and B are same. It is because the cloud contribution and the scattering process are both ignored in equation (8). Given the simplicity of equation (8), the estimates agree reasonably well with the retrieval.

[35] To assess the applicability of equation (8), we extended the case A to other optical thicknesses from 0.1 to 7, while holding the r_e at cloud top and base constantly to 15 and 45 μm , respectively. Figure 8a shows how the $\Delta\varepsilon_{ap} = \varepsilon_{ap}(8.5\ \mu\text{m}) - \varepsilon_{ap}(11\ \mu\text{m})$ (solid line) and the corresponding $w_{\Delta\varepsilon}$ of surface (dashed line) vary with the τ_c of the ice cloud

above it. As discussed previously, a positive $\Delta\varepsilon_{ap}$ is due to the weaker cloud absorption (stronger surface transmission) at the 8.5 μm than at the 11 μm . The $\Delta\varepsilon_{ap}$ decreases with increasing τ_c , because the increasing cloud absorption decreases the signal from the surface. When the ice cloud is very thin, the $w_{\Delta\varepsilon}$ of the surface approaches unity, indicating a negligible cloud impact on $\Delta\varepsilon_{ap}$ for the very thin ice clouds. As τ_c increases, the value of surface $w_{\Delta\varepsilon}$ continues to increase and becomes larger than unity. This is a result of the increasing negative impact of cloud emission. Roughly speaking, the impact of the cloud on $\Delta\varepsilon_{ap}$ and therefore r_e^* remains relatively small, in comparison with the surface, for τ_c smaller than about 5. Figure 8b shows the comparison between the retrieved r_e^* and the estimated r_e^* based on equation (8) which was only intended to be valid over that optical thickness range. Evidently, the estimates agree reasonably well with the retrievals for small τ_c , but deviate further away from the retrievals as the impact of cloud emission increases. It should be pointed out that, owing to the loss of sensitivity (see Figure 3), the IRSpW algorithm becomes highly sensitive to the numerical errors for τ_c larger than 5. For these clouds, first-guess values of τ_c and r_e^* were used to avoid erroneous retrievals.

[36] To conclude, when the ice cloud is moderately optically thick, the IRSpW method is relatively insensitive to cloud vertical structure and effective radius retrieval is weighted toward smaller ice particle size, while the weighting function makes the SRBS method more sensitive to the ice particle size in the upper portion of the cloud. As a result, when ice particle size increases monotonically toward cloud base, the two methods are in qualitative agreement; in the event that ice particle size decreases toward cloud base, the effective radius and ice water path retrievals based on the SRBS method are substantially larger than those from the IRSpW.

4.3. Consistency Between the SRBS and IRSpW Method: A Model Case Study

[37] In sections 4.1 and 4.2, we gained a physical understanding of how ice particle size vertical inhomogeneity can lead to different cloud property retrievals between SRBS and IRSpW methods. In this section we test the robustness of these findings with more realistic ice cloud vertical r_e profiles from model simulations. The model used here is a one-dimensional time-dependent cirrus cloud simulation model. It was originally developed by Lin *et al.* [2005] and modified by Comstock *et al.* [2008]. The simulation shown here was forced by remote sensing measurements obtained at the Department of Energy's Southern Great Plains (SGP) Atmospheric Radiation Measurement (ARM) site on 7 December 1999 [Comstock *et al.*, 2008]. It has been shown that the simulated cloud evolution and bulk properties agree reasonably well with observations [Comstock *et al.*, 2008].

[38] Figure 9a shows the evolution of the vertical IWC profile of the simulated cirrus cloud. The vertical profile of r_e in the optical depth coordinate at hours 4, 5, and 6 (marked as the dashed lines in Figure 9a) are shown in Figures 9b, 9c, and 9d, respectively. Note that these three profiles represent three different combinations of ice cloud optical thickness (see Figure 10) and vertical r_e variation. At hour 4, the ice cloud is optically thin (~ 0.5) and yet has a

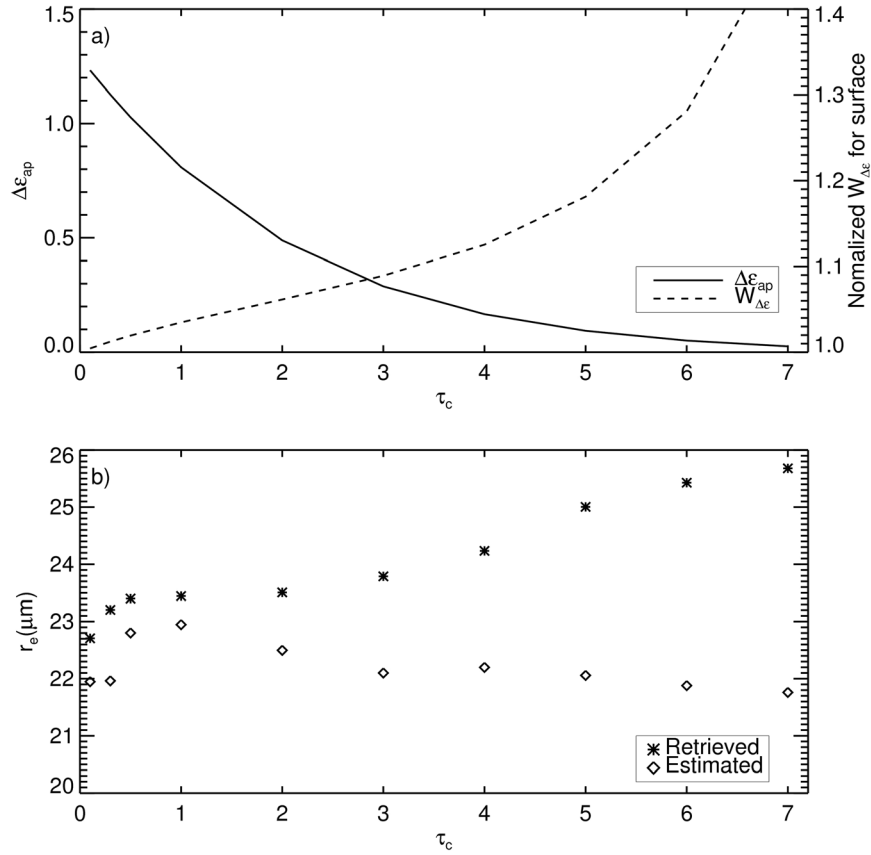


Figure 8. (a) Variation of $\Delta\epsilon_{ap} = \epsilon_{ap}(8.5\mu\text{m}) - \epsilon_{ap}(11\mu\text{m})$ (solid line) and the corresponding $w_{\Delta\epsilon}$ of surface (dashed line) with the optical thickness of the ice cloud above it. The ice cloud is assumed to be vertically inhomogeneous with effective radius increasing linearly with optical depth from $15\mu\text{m}$ at cloud top to $45\mu\text{m}$ at cloud base. (b) Comparison of the retrieved effective radius and estimated value based on equation (8).

large vertical r_e gradient. At hour 5, the ice cloud is moderately thick (~ 2.5), but also with a large variation of r_e . At hour 6, the ice cloud is thin (~ 0.4) and rather homogenous. On the basis of such profiles, we first simulated the satellite-observed radiances at all relevant wavelengths using the DISORT model. For simplicity, a constant 45° solar zenith angle was used for the entire simulation period and the cloud temperature was specified uniformly at 230 K. On the basis of the simulated radiances, τ_c^* , r_e^* , and IWP^* were then retrieved using SRBS and the IRSpW algorithms with different combinations of wavelengths.

[39] Figure 10 (top) shows the τ_c^* retrieval comparisons. Similar to the two simple simulated cases discussed earlier (see Table 1), τ_c^* retrievals from different methods are in close agreement with each other. Once again, this result indicates that the vertical structure of the ice cloud has only a very limited impact on the optical thickness retrieval. This is consistent with the finding in the work of Yang *et al.* [2001] that the visible channel is not sensitive to ice cloud inhomogeneity. Figure 10 (middle) shows comparisons between r_e^* retrievals based on the SRBS (blue lines) and IRSpW (red lines) methods. For comparison, the optical depth weighted effective radius that gives the correct IWP, $\bar{r}_e = \int_0^{\tau_c} r_e(\tau) d\tau / \tau_c$, (solid black line) derived from the

simulated $r_e(\tau)$ profile is also plotted. Overall, the r_e^* retrieval results are in accordance with expectations from the vertical profiles. During the first few hours, for example at hour 4 (Figure 9b), the simulated ice cloud is optically thin and yet has a large vertical r_e gradient from cloud top toward cloud base. For the reasons discussed in section 4.1, the retrievals based on the IRSpW method are significantly smaller than those based on the SRBS method which still underestimates \bar{r}_e . At hour 5, the ice cloud has gained a moderate optical thickness of about 3. It has a large vertical r_e gradient, with the cloud top value of only a few microns and a maximum value of more than 90 microns close to cloud base. For such a cloud structure, as discussed earlier, the r_e^* retrieval based on the SRBS method is weighted toward the cloud top value, while the IRSpW method is more sensitive to small ice particles. This explains the reasonable agreement between the two methods at this time, except for $r_e^*(3.7\mu\text{m})$ which is, also as expected, substantially smaller than the others. During the later part of the simulation, for example at hour 6, the simulated ice cloud becomes optically thin again and, more importantly, relatively homogeneous, explaining the close agreement between different r_e^* retrievals. Figure 10 (bottom) shows the IWP comparison. As expected, both methods underes-

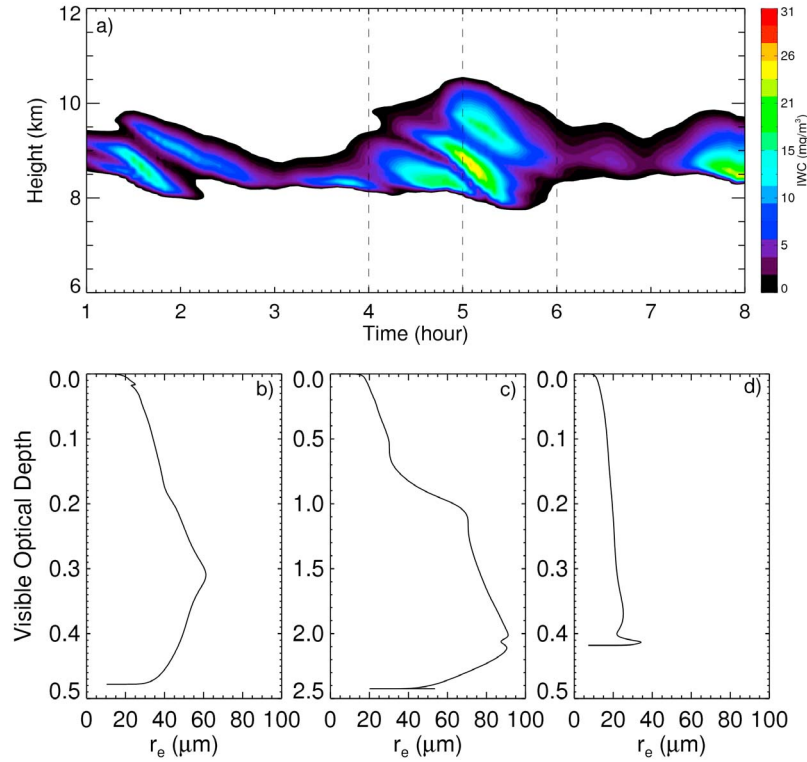


Figure 9. A cirrus cloud simulated by a single-column model [Comstock *et al.*, 2008]. (a) Evolution of the vertical IWC profile of the simulated cirrus cloud. The vertical profiles of r_e in optical depth space are shown at (b) 4, (c) 5, and (d) 6 h of the simulation.

timate the simulation and the IWP difference follows closely the r_e^* retrievals in Figure 10 (middle).

5. Summary and Discussion

[40] The SRBS and IRSpW methods have been extensively used for retrieving cloud τ_c and r_e from observations made by multispectral satellite imagers. There is a pressing need to compare and evaluate cloud property retrievals using the two methods. The integration of retrievals based on different parts of the spectrum also provides an opportunity to better establish a long-term imager-based global data set of ice cloud optical and microphysical properties, which is invaluable for improving climatologies and the representation of ice clouds in climate models. However, fundamental questions must be addressed before comparing and/or combining the retrieval approaches.

[41] Although most ice clouds are vertically inhomogeneous to some extent, current operational, global algorithms based on the SRBS and IRSpW methods assume that the observed cloud is homogenous. In this study, we investigated whether this assumption could lead to discrepancies between the two methods. Note that the retrieved cloud particle effective radius based on homogenous assumption is referred to as r_e^* in this study for the sake of clarity. The main findings can be summarized as follows:

[42] 1. When an ice cloud is optically thin and yet has a significant vertical variation in r_e , the cloud particle effective radius retrieval under the homogenous assumption amounts to an interpolation problem. The radiative properties of ice clouds (for example ω in the SWIR spectral region

and ΔQ_a between two IR wavelengths, which are the key variables for the r_e^* retrievals based on the SRBS and IRSpW methods, respectively) vary nonlinearly with ice particle effective radius. As a result, in both methods the retrieval under the homogenous cloud assumption tends to give r_e^* retrievals smaller than the optical depth weighted average; that is, $r_e^* < \bar{r}_e = \int_0^{\tau_c} r_e(\tau) d\tau / \tau_c$. Because the dependence of ΔQ_a on r_e is generally more nonlinear than that for SWIR ω , the r_e^* based on the IRSpW method tends to be smaller than that based on the SRBS method (see Figures 4 and 10).

[43] 2. Consistent with previous studies [Platnick, 2000], we found that when the ice cloud has a moderate optical thickness the r_e^* retrieval based the SRBS method is weighted toward the r_e value close to cloud top (see Figure 5). Utilizing the new concept of an apparent emissivity weighting function, we discovered a compensating mechanism that limits the contribution of cloud emission to the r_e^* signal (see Figure 7 and the analysis in section 4.2). Because only small ice particles exhibit significant Q_a difference between any two of the IR wavelengths considered, while the Q_a of large ice particles are rather spectrally flat, the signal for r_e^* in the IRSpW method is contributed mostly by surface emission transmitted through the ice cloud and is more sensitive to the small ice particles than the larger ones. Taken the inherent sensitivities of the two methods together, we found that when r_e increases from cloud top toward cloud base, r_e^* based on the two methods are in qualitative agreement. On the other hand, when r_e decreases from cloud top toward cloud base, r_e^* based on the SRBS method is substantially larger than that based on the IRSpW method.

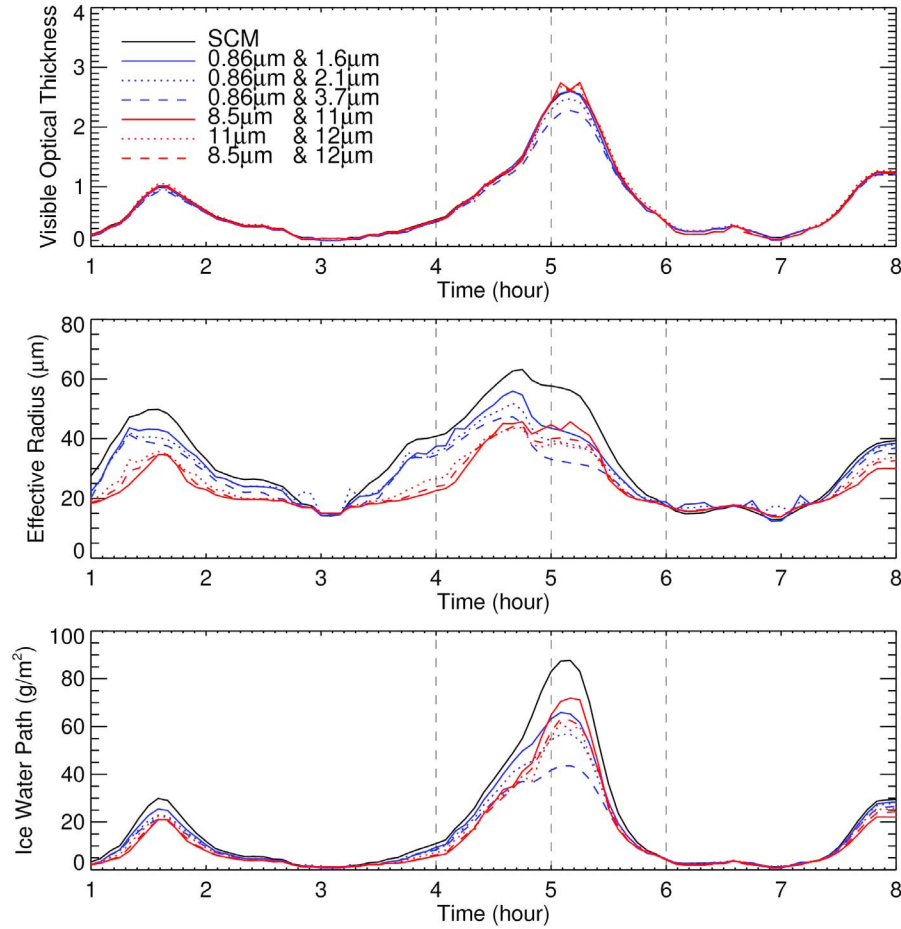


Figure 10. The (top) τ_c^* , (middle) r_c^* , and (bottom) IWP retrieved using different methods and different combinations of wavelengths in comparison with the 1-D model simulation.

[44] 3. In both simple prescribed cases (see Table 1) and the more realistic and complex cases (Figure 10), we found only very limited impact of the size vertical inhomogeneity on τ_c^* retrievals using either method. Therefore, in both methods, the error in IWP retrievals caused by the homogeneous cloud assumption follows closely with the difference between r_c^* and $\bar{r}_c = \int_0^{\tau_c} r_c(\tau) d\tau / \tau_c$. Depending on the optical thickness of the ice cloud and the vertical structure of r_c , the IWP retrievals based on the two methods can be significantly different.

[45] The above findings have several implications for the remote sensing of ice cloud properties and the use of these retrieved properties in model validation and parameterization. First of all, they suggest to us the existence of a potential significant bias in current IWP retrievals, caused by the homogeneous cloud assumption. The existence of such a bias in water cloud retrievals has been well recognized and documented [e.g., Nakajima and King, 1990; Plattnick, 2000]. In fact, some attempts have already been made recently to eliminate such bias by incorporating a vertical structure assumption into water cloud retrieval algorithms (e.g., adiabatic [e.g., Brenguier et al., 2000; Chang and Li, 2002, 2003; Schuller et al., 2003; Bennartz, 2007] and effective radius linear with physical thickness [Chang and Li, 2002, 2003]). Unfortunately, little is yet known about such bias in ice cloud

retrievals, although studies such as the present one indicate the potential importance. The reason for the current situation is the lack of reliable in situ measurements of ice effective particle radius vertical structure collocated with remote sensing measurements of the same cloud, coupled with the fact that processes which controls the generation, growth, and fall speed of ice particles are more complicated than those in water clouds. This makes it exceedingly difficult to establish a simple conceptual model, analogous to the adiabatic growth model for water droplets for example, to predicate a nominal vertical structure for which to estimate the error caused by a homogeneous cloud assumption. The above findings also suggest that caution should be taken when comparing the ice cloud property retrievals between the SRBS and IRSpW methods. The vertical inhomogeneity of ice clouds may lead to significant discrepancy between the two methods, even if they are applied to the same cloud and other uncertainties are well constrained. In this sense, even a close agreement between the two methods needs to be examined and interpreted carefully. On the other hand, the differences in effective radius retrievals between different bands and methods also provide useful information about cloud vertical structures. Some recent studies have shown the possibility to achieve better understanding of cloud vertical structure through a careful combination of difference

bands or methods [Chang and Li, 2002, 2003; Ehrlich et al., 2009; Wang et al., 2009; Seethala and Horváth, 2010].

[46] Finally, we point out that our effort focused specifically on cloud vertical inhomogeneity effects, we ignored all other physical uncertainties inherent to the retrievals, for example, uncertainties in cloud top temperature (IRSpW), atmospheric emission (IRSpW) and absorption (IRSpW, SRBS), surface reflectance and emissivity (SRBS, IRSpW), and ice particle habit distributions (SRBS, IRSpW). The latter three uncertainty sources are usually provided from modeled or observation-based ancillary data sets. Uncertainties associated with the specification of these values may have a significant impact on the retrievals. More importantly, they may affect the SRBS and IRSpW methods to different extents and therefore lead to retrieval differences beyond that due to vertical inhomogeneities alone. Further work is needed to identify the relative importance of the uncertainty caused by the homogenous cloud assumption and other error sources, such as the vertical temperature variation, that are inherent to the retrieval algorithms, in addition to observational case studies with MODIS and/or equivalent airborne imagers.

Appendix A: Weighting Functions for the IR Split-Window Method

[47] Following [Platnick, 2000], we divide the cloud and surface contributions to the observed radiance (specifically ε_{ap} in this study) into two separate parts. The source terms correspond to thermal emission from a cloud sublayer or the surface. The other term is the so-called escape function (E) for in-cloud layers. The physical interpretation of E is that it gives the amount of radiation that escapes at cloud top from a unit source located within the cloud. In terms of the escape function, the infrared radiative transfer equation can be written as:

$$\varepsilon_{ap}(\lambda) = \int_0^{\tau_c} Q_a[\lambda, r_e(\tau)] E[\lambda, r_e(\tau)] d\tau + \varepsilon_s \frac{B(\lambda, T_s)}{B(\lambda, T_c)} E(\lambda, surf), \quad (A1)$$

where Q_a is the absorption efficiency, ε_s denotes the surface emissivity, B is the Planck function, and T_s and T_c are the surface and cloud temperature (assumed to be homogenous in this study). Note that in the literature, the escape function is also referred to as the “response function” [Marchuk, 1964; Box et al., 1988; Box, 2002] or the “Green’s function” [Twomey, 1985]. To compute $E(\lambda, \tau)$, we first discretize the inhomogeneous ice cloud into, say, N sublayers with the same visible optical thickness. Each sublayer is assumed to be homogeneous. Admittedly, the optical thickness of each sublayer at different IR wavelengths may be different because of the difference of r_e . The visible optical thickness space is, nevertheless, used to provide a common base for comparison between different IR wavelengths. The escape function for each sublayer of the ice cloud ($E(\lambda, \tau_i)$) and the surface ($E(\lambda, surf)$) are computed utilizing the principle of reciprocity [Marchuk, 1964; Box et al., 1988; Box, 2002]. Specifically, we first specify an adjoint source [Box et al., 1988] at the top of atmosphere in the backward direction of the satellite-viewing direction. Then, we compute the net radiation flux (normalized by the adjoint source)

induced by this adjoint source at each sublayer of the cloud and also at the surface, which, according to the principle of reciprocity, corresponds to the escape function for each sublayer or the surface. The computations are carried out using the DISORT model described in [Stamnes et al., 1988]. After $E(\lambda, \tau_i)$ is obtained, the normalized weighting function, $C(\lambda, \tau_i)$, for each sublayer i can be derived from

$$w_\varepsilon(\lambda, \tau_i, \Delta\tau) = \frac{Q_a[\lambda, r_e(\tau_i)] E(\lambda, \tau_i) \Delta\tau}{\varepsilon_{ap}(\lambda)}. \quad (A2)$$

The normalized weighting function from the surface is

$$w_\varepsilon(\lambda, surf) = \frac{\varepsilon_s B(\lambda, T_s)}{B(\lambda, T_s)} \frac{E(\lambda, surf)}{\varepsilon_{ap}(\lambda)}. \quad (A3)$$

After the normalization, the weighting function $w_\varepsilon(\lambda, \tau_c)$ satisfies

$$\sum_{i=1}^N w_\varepsilon(\lambda, \tau_i) + w_\varepsilon(\lambda, surf) = 1. \quad (A4)$$

In a similar way, we can also derive the contribution function for $\Delta\varepsilon_{ap}$. We rewrite $\Delta\varepsilon_{ap}(\lambda_1, \lambda_2)$ as

$$\begin{aligned} \Delta\varepsilon_{ap}(\lambda_1, \lambda_2) &= [K_s(\lambda_1) E(\lambda_1, surf) - K_s(\lambda_2) E(\lambda_2, surf)] \\ &+ \int_0^{\tau_c} \{Q_a[\lambda, r_e(\tau)] E(\lambda_1, \tau) - Q_a[\lambda, r_e(\tau)] E(\lambda_2, \tau)\} d\tau, \end{aligned} \quad (A5)$$

where $K_s = \varepsilon_s B(\lambda, T_s)/B(\lambda, T_c)$. Then the weighting function of each sublayer i is simply

$$\begin{aligned} w_{\Delta\varepsilon}(\lambda_1, \lambda_2, \tau_i, \Delta\tau) &= \frac{\{Q_a[\lambda, r_e(\tau)] E(\lambda_1, \tau_i) - Q_a[\lambda, r_e(\tau)] E(\lambda_2, \tau_i)\} \Delta\tau}{\Delta\varepsilon_{ap}(\lambda_1, \lambda_2)}, \end{aligned} \quad (A6)$$

and the contribution function for the surface is

$$w_{\Delta\varepsilon}(\lambda_1, \lambda_2, surf) = \frac{[K_s(\lambda_1) E(\lambda_1, surf) - K_s(\lambda_2) E(\lambda_2, surf)]}{\Delta\varepsilon_{ap}(\lambda_1, \lambda_2)}. \quad (A7)$$

Note that the calculated weighting functions for each cloud sublayer, $w_\varepsilon(\lambda, \tau_i, \Delta\tau)$ and $w_{\Delta\varepsilon}(\lambda_1, \lambda_2, \tau_i, \Delta\tau)$, are dependent on the resolution of the discretization; that is, $d\tau$. In all computations, $d\tau$ was specified as 0.1.

[48] **Acknowledgments.** This work was funded in part by NASA’s Radiation Sciences Program. P. Yang acknowledges NASA support (NNX08AP57G). The contribution from J. M. Comstock was supported by the DOE Atmospheric Radiation Measurement Program. The authors thank the two reviewers for their insightful comments, questions, and suggestions, which have helped to improve this manuscript.

References

- Ackerman, S. A., W. L. Smith, H. E. Revercomb, and J. D. Spinhirne (1990), The 27–28 October 1986 FIRE IFO Cirrus case study: Spectral properties of cirrus clouds in the 8–12 μm window, *Mon. Weather Rev.*, 118, 2377–2388, doi:10.1175/1520-0493(1990)118<2377:TOFICC>2.0.CO;2.

- Ackerman, S. A., K. I. Strabala, W. P. Menzel, R. A. Frey, C. C. Moeller, and L. E. Gumley (1998), Discriminating clear sky from clouds with MODIS, *J. Geophys. Res.*, **103**, 132,141–132,157.
- Ackerman, T. P., K.-N. Liou, F. P. J. Valero, and L. Pfister (1988), Heating rates in tropical anvils, *J. Atmos. Sci.*, **45**, 1606–1623, doi:10.1175/1520-0469(1988)045<1606:HRITA>2.0.CO;2.
- Baum, B., K. I. Strabala, S. A. Ackerman, M. D. King, W. P. Menzel, P. F. Soulen, and P. Yang (2000), Remote sensing of cloud properties using MODIS airborne simulator imagery during SUCCESS: 2. Cloud thermodynamic phase, *J. Geophys. Res.*, **105**, 11,781–11,792, doi:10.1029/1999JD901090.
- Baum, B., P. Yang, A. Heymsfield, and S. Thomas (2005a), Bulk scattering properties for the remote sensing of ice clouds. part I: Microphysical data and models, *J. Appl. Meteorol.*, **44**, 1885–1895, doi:10.1175/JAM2308.1.
- Baum, B., P. Yang, A. J. Heymsfield, S. Platnick, M. D. King, Y. X. Hu, and S. T. Bedka (2005b), Bulk scattering properties for the remote sensing of ice clouds. part II: Narrowband models, *J. Appl. Meteorol.*, **44**, 1896–1911, doi:10.1175/JAM2309.1.
- Bennartz, R. (2007), Global assessment of marine boundary layer cloud droplet number concentration from satellite, *J. Geophys. Res.*, **112**, D02201, doi:10.1029/2006JD007547.
- Box, M. A. (2002), Radiative perturbation theory: A review, *Environ. Modell. Software*, **17**, 95–106, doi:10.1016/S1364-8152(01)00056-1.
- Box, M. A., S. A. W. Gerstl, and C. Simmer (1988), Application of the adjoint formulation to the calculation of atmospheric radiative effects, *Beitr. Phys. Atmos.*, **61**, 303–311.
- Brenguier, J.-L., H. Pawlowska, L. Schüller, R. Preusker, and J. Fischer (2000), Radiative properties of boundary layer clouds: Droplet effective radius versus number concentration, *J. Atmos. Sci.*, **57**, 803–821, doi:10.1175/1520-0469(2000)057<0803:RPOBLC>2.0.CO;2.
- Chandrasekhar, S. (1960), *Radiative Transfer*, Dover Publ., New York.
- Chang, F.-L., and Z. Li (2002), Estimating the vertical variation of cloud droplet effective radius using multispectral near-infrared satellite measurements, *J. Geophys. Res.*, **107**(D15), 4257, doi:10.1029/2001JD000766.
- Chang, F.-L., and Z. Li (2003), Retrieving vertical profiles of water-cloud droplet effective radius: Algorithm modification and preliminary application, *J. Geophys. Res.*, **108**(D24), 4763, doi:10.1029/2003JD003906.
- Chung, S., S. Ackerman, P. F. van Delst, and W. P. Menzel (2000), Model calculations and interferometer measurements of ice-cloud characteristics, *J. Appl. Meteorol.*, **39**, 634–644.
- Comstock, J. M., R. d'Entremont, D. DeSlover, G. G. Mace, S. Y. Matrosov, S. A. McFarlane, P. Minnis, D. Mitchell, K. Sassen, and M. D. Shupe (2007), An intercomparison of microphysical retrieval algorithms for upper-tropospheric ice clouds, *Bull. Am. Meteorol. Soc.*, **88**, 191–204, doi:10.1175/BAMS-88-2-191.
- Comstock, J. M., R.-F. Lin, D. O'C. Starr, and P. Yang (2008), Understanding ice supersaturation, particle growth, and number concentration in cirrus clouds, *J. Geophys. Res.*, **113**, D23211, doi:10.1029/2008JD010332.
- Cooper, S. J., T. S. L'Ecuyer, and G. L. Stephens (2003), The impact of explicit cloud boundary information on ice cloud microphysical property retrievals from infrared radiances, *J. Geophys. Res.*, **108**(D3), 4107, doi:10.1029/2002JD002611.
- Ehrlich, A., M. Wendisch, E. Bierwirth, J. F. Gayet, G. Mioche, A. Lampert, and B. Mayer (2009), Evidence of ice crystals at cloud top of Arctic boundary-layer mixed-phase clouds derived from airborne remote sensing, *Atmos. Chem. Phys.*, **9**, 9401–9416, doi:10.5194/acp-9-9401-2009.
- Foot, J. S. (1988), Some observations of the optical properties of clouds. II: Cirrus, *Q. J. R. Meteorol. Soc.*, **114**, 145–164, doi:10.1002/qj.49711447908.
- Francis, P. N., A. Jones, R. W. Saunders, K. P. Shine, A. Slingo, and Z. Sun (1994), An observational and theoretical study of the radiative properties of cirrus: Some results from ICE'89, *Q. J. R. Meteorol. Soc.*, **120**, 809–848, doi:10.1002/qj.49712051804.
- Fu, Q., and K. N. Liou (1993), Parameterization of the radiative properties of cirrus clouds, *J. Atmos. Sci.*, **50**, 2008–2025, doi:10.1175/1520-0469(1993)050<2008:POTRPO>2.0.CO;2.
- Han, Q., W. B. Rossow, and A. A. Lacis (1994), Near global survey of effective droplet radii in liquid clouds using ISCCP data, *J. Clim.*, **7**, 465–497, doi:10.1175/1520-0442(1994)007<0465:NGSOED>2.0.CO;2.
- Hartmann, D. L., M. E. Ockert-Bell, and M. L. Michelsen (1992), The effect of cloud type on Earth's energy balance: Global analysis, *J. Clim.*, **5**, 1281–1304, doi:10.1175/1520-0442(1992)005<1281:TEOCTO>2.0.CO;2.
- Heidinger, A. K., and M. J. Pavolonis (2009), Gazing at cirrus clouds for 25 years through a split window. part I: Methodology, *J. Appl. Meteorol. Climatol.*, **48**, 1100–1116, doi:10.1175/2008JAMC1882.1.
- Heymsfield, A. J., A. Bansemer, P. R. Field, S. L. Durden, J. L. Stith, J. E. Dye, W. Hall, and C. A. Grainger (2002), Observations and parameterizations of particle size distributions in deep tropical cirrus and stratiform precipitating clouds: Results from in situ observations in TRMM field campaigns, *J. Atmos. Sci.*, **59**, 3457–3491, doi:10.1175/1520-0469(2002)059<3457:OAPOPS>2.0.CO;2.
- Heymsfield, A. J., C. Schmitt, A. Bansemer, G.-J. van Zadelhoff, M. J. McGill, C. Twohy, and D. Baumgardner (2006), Effective radius of ice cloud particle populations derived from aircraft probes, *J. Atmos. Oceanic Technol.*, **23**, 361–380, doi:10.1175/JTECH1857.1.
- Huang, H.-L., P. Yang, H. Wei, B. A. Baum, Y. Hu, P. Antonelli, and S. A. Ackerman (2004), Inference of ice cloud properties from high spectral resolution infrared observations, *IEEE Trans. Geosci. Remote Sens.*, **42**, 842–853, doi:10.1109/TGRS.2003.822752.
- Inoue, T. (1985), On the temperature and effective emissivity determination of semi-transparent cirrus clouds by bi-spectral measurements in the 10 micron window region, *J. Meteorol. Soc. Jpn.*, **63**, 88–99.
- Inoue, T. (1987), A cloud type classification with NOAA 7 split-window measurements, *J. Geophys. Res.*, **92**, 3991–4000, doi:10.1029/JD092iD04p03991.
- Jensen, E. J., S. Kinne, and O. B. Toon (1994), Tropical cirrus cloud radiative forcing—Sensitivity studies, *Geophys. Res. Lett.*, **21**, 2023–2026, doi:10.1029/94GL01358.
- Kokhanovsky, A. A. (2004), The depth of sunlight penetration in cloud fields for remote sensing, *IEEE Geosci. Remote Sens. Lett.*, **1**, 242–245, doi:10.1109/LGRS.2004.832228.
- Lin, R.-F., D. O. Starr, J. Reichardt, and P. J. DeMott (2005), Nucleation in synoptically forced cirrostratus, *J. Geophys. Res.*, **110**, D08208, doi:10.1029/2004JD005362.
- Liou, K.-N. (1986), Influence of cirrus clouds on weather and climate processes: A global perspective, *Mon. Weather Rev.*, **114**, 1167–1199, doi:10.1175/1520-0493(1986)114<1167:IOCCOW>2.0.CO;2.
- Marchuk, G. I. (1964), Equation for the value of information from weather satellites and formulation of inverse problems, *Cosmic Res., Engl. Transl.*, **2**, 394–408.
- Marshak, A., S. Platnick, T. Várnai, G. Wen, and R. F. Cahalan (2006), Impact of three-dimensional radiative effects on satellite retrievals of cloud droplet sizes, *J. Geophys. Res.*, **111**, D09207, doi:10.1029/2005JD006686.
- Martin, G. M., D. W. Johnson, and A. Spice (1994), The measurement and parameterization of effective radius of droplets in warm stratocumulus clouds, *J. Atmos. Sci.*, **51**, 1823–1842, doi:10.1175/1520-0469(1994)051<1823:TMAPOE>2.0.CO;2.
- Masuda, K., T. Takashima, and Y. Takayama (1988), Emissivity of pure and sea waters for the model sea surface in the infrared window regions, *Remote Sens. Environ.*, **24**, 313–329, doi:10.1016/0034-4257(88)90032-6.
- McFarquhar, G. M., and A. J. Heymsfield (1998), The definition and significance of an effective radius for ice clouds, *J. Atmos. Sci.*, **55**, 2039–2052, doi:10.1175/1520-0469(1998)055<2039:TDASOA>2.0.CO;2.
- Miles, N. L., J. Verlinde, and E. E. Clothiaux (2000), Cloud droplet size distributions in low-level stratiform clouds, *J. Atmos. Sci.*, **57**, 295–311, doi:10.1175/1520-0469(2000)057<0295:CDSOIL>2.0.CO;2.
- Miller, S. D., J. D. Hawkins, J. Kent, F. J. Turk, T. F. Lee, A. P. Kuciauskas, K. Richardson, R. Wade, and C. Hoffman (2006), NexSat: Previewing NPOESS/VIIRS imagery capabilities, *Bull. Am. Meteorol. Soc.*, **87**, 433–446, doi:10.1175/BAMS-87-4-433.
- Nakajima, T., and M. D. King (1990), Determination of the optical thickness and effective particle radius of clouds from reflected solar radiation measurements. part I: Theory, *J. Atmos. Sci.*, **47**, 1878–1893, doi:10.1175/1520-0469(1990)047<1878:DOTOTA>2.0.CO;2.
- Nakajima, T., and T. Nakajima (1995), Wide-area determination of cloud microphysical properties from NOAA AVHRR measurements for FIRE and ASTEX regions, *J. Atmos. Sci.*, **52**, 4043–4059, doi:10.1175/1520-0469(1995)052<4043:WADOCM>2.0.CO;2.
- Oreopoulos, L., and R. Davies (1998), Plane parallel albedo biases from satellite observations. part I: Dependence on resolution and other factors, *J. Clim.*, **11**, 919–932, doi:10.1175/1520-0442(1998)011<0919:PPABFS>2.0.CO;2.
- Parol, F., J. C. Buriez, G. Brogniez, and Y. Fouquart (1991), Information content of AVHRR channels 4 and 5 with respect to the effective radius of cirrus cloud particles, *J. Appl. Meteorol.*, **30**, 973–984.
- Platnick, S. (2000), Vertical photon transport in cloud remote sensing problems, *J. Geophys. Res.*, **105**, 22,919–22,935, doi:10.1029/2000JD900333.
- Platnick, S., and S. Twomey (1994), Determining the susceptibility of cloud albedo to changes in droplet concentration with the Advanced

- Very High Resolution Radiometer, *J. Appl. Meteorol.*, **33**, 334–347, doi:10.1175/1520-0450(1994)033<0334:DTSOCA>2.0.CO;2.
- Platnick, S., and F. P. J. Valero (1995), A validation of a satellite cloud retrieval during ASTEX, *J. Atmos. Sci.*, **52**, 2985–3001, doi:10.1175/1520-0469(1995)052<2985:AVOASC>2.0.CO;2.
- Platnick, S., P. A. Durkee, K. Nielsen, J. P. Taylor, S. C. Tsay, M. D. King, R. J. Ferek, P. V. Hobbs, and J. W. Rottman (2000), The role of background cloud microphysics in the radiative formation of ship tracks, *J. Atmos. Sci.*, **57**, 2607–2624, doi:10.1175/1520-0469(2000)057<2607:TROBCM>2.0.CO;2.
- Platnick, S., M. D. King, S. A. Ackerman, W. P. Menzel, B. A. Baum, J. C. Riedi, and R. A. Frey (2003), The MODIS cloud products: Algorithms and examples from Terra, *IEEE Trans. Geosci. Remote Sens.*, **41**, 459–473, doi:10.1109/TGRS.2002.808301.
- Prabhakara, C., R. S. Fraser, G. Dalu, M.-L. C. Wu, R. J. Curran, and T. Styles (1988), Thin cirrus clouds: Seasonal distribution over oceans deduced from Nimbus-4 IRIS, *J. Appl. Meteorol.*, **27**, 379–399, doi:10.1175/1520-0450(1988)027<0379:TCCSDO>2.0.CO;2.
- Pruppacher, H., and J. Klett (1997), *Microphysics of Clouds and Precipitation*, Kluwer Acad., Boston, Mass.
- Ramanathan, V., R. D. Cess, E. F. Harrison, P. Minnis, B. R. Barkstrom, E. Ahmad, and D. Hartmann (1989), Cloud-radiative forcing and climate: Results from the Earth Radiation Budget Experiment, *Science*, **243**, 57–63, doi:10.1126/science.243.4887.57.
- Roebeling, R. A., A. J. Feijt, and P. Stammes (2006), Cloud property retrievals for climate monitoring: Implications of differences between Spinning Enhanced Visible and Infrared Imager (SEVIRI) on METEOSAT-8 and Advanced Very High Resolution Radiometer (AVHRR) on NOAA-17, *J. Geophys. Res.*, **111**, D20210, doi:10.1029/2005JD006990.
- Rozanov, V. V., and A. A. Kokhanovsky (2005), The average number of photon scattering events in vertically inhomogeneous atmosphere, *J. Quant. Spectrosc. Radiat. Transfer*, **97**, 11–13.
- Schmit, T. J., M. M. Gunshor, W. P. Menzel, J. J. Gurka, J. Li, and A. S. Bachmeier (2005), Introducing the next-generation Advanced Baseline Imager on GOES-R, *Bull. Am. Meteorol. Soc.*, **86**, 1079–1096, doi:10.1175/BAMS-86-8-1079.
- Schüller, L., J.-L. Brenguier, and H. Pawlowska (2003), Retrieval of microphysical, geometrical, and radiative properties of marine stratocumulus from remote sensing, *J. Geophys. Res.*, **108**(D15), 8631, doi:10.1029/2002JD002680.
- Seethala, C., and Á. Horváth (2010), Global assessment of AMSR-E and MODIS cloud liquid water path retrievals in warm oceanic clouds, *J. Geophys. Res.*, **115**, D13202, doi:10.1029/2009JD012662.
- Sherwood, S. C. (2002), Aerosols and ice particle size in tropical cumulonimbus, *J. Clim.*, **15**, 1051–1063, doi:10.1175/1520-0442(2002)015<1051:AAIPSI>2.0.CO;2.
- Stammes, K., S. C. Tsay, K. Jayaweera, and W. Wiscombe (1988), Numerically stable algorithm for discrete-ordinate-method radiative transfer in multiple scattering and emitting layered media, *Appl. Opt.*, **27**, 2502–2509, doi:10.1364/AO.27.002502.
- Strabala, K. I., S. A. Ackerman, and W. P. Menzel (1994), Cloud properties inferred from 8–12- μm data, *J. Appl. Meteorol.*, **33**, 212–229, doi:10.1175/1520-0450(1994)033<0212:CPIFD>2.0.CO;2.
- Twomey, S. (1985), Green's function formulae for the internal intensity in radiative transfer computations by matrix-vector methods, *J. Quant. Spectrosc. Radiat. Transfer*, **33**, 575–579.
- van de Hulst, H. C. (1957), *Light Scattering by Small Particles*, John Wiley, New York.
- Waliser, D. E., et al. (2009), Cloud ice: A climate model challenge with signs and expectations of progress, *J. Geophys. Res.*, **114**, D00A21, doi:10.1029/2008JD010015.
- Wang, X., K. N. Liou, S. S. C. Ou, G. G. Mace, and M. Deng (2009), Remote sensing of cirrus cloud vertical size profile using MODIS data, *J. Geophys. Res.*, **114**, D09205, doi:10.1029/2008JD011327.
- Warren, S. G. (1984), Optical constants of ice from the ultraviolet to the microwave, *Appl. Opt.*, **23**, 1206–1225, doi:10.1364/AO.23.001206.
- Webb, M. J., C. A. Senior, D. M. H. Sexton, W. J. Ingram, K. D. Williams, M. A. Ringer, B. J. McAvaney, R. Colman, B. J. Soden, and R. Guedel (2006), On the contribution of local feedback mechanisms to the range of climate sensitivity in two GCM ensembles, *Clim. Dyn.*, **27**, 17–38, doi:10.1007/s00382-006-0111-2.
- Yang, P., K. N. Liou, K. Wyser, and D. Mitchell (2000), Parameterization of the scattering and absorption properties of individual ice crystals, *J. Geophys. Res.*, **105**, 4699–4718, doi:10.1029/1999JD900755.
- Yang, P., W. J. Wiscombe, P. F. Soulen, B. C. Gao, B. A. Baum, Y. X. Hu, S. L. Nasiri, A. J. Heymsfield, G. M. McFarquhar, and L. M. Miloshevich (2001), Sensitivity of cirrus bidirectional reflectance to vertical inhomogeneity of ice crystal habits and size distributions for two Moderate-Resolution Imaging Spectroradiometer (MODIS) bands, *J. Geophys. Res.*, **106**, 17,267–17,291.
- Yang, P., H. Wei, H.-L. Huang, B. A. Baum, Y. X. Hu, G. W. Kattawar, M. I. Mishchenko, and Q. Fu (2005), Scattering and absorption property database for nonspherical ice particles in the near- through far-infrared spectral region, *Appl. Opt.*, **44**, 5512–5523, doi:10.1364/AO.44.005512.
- Zhang, M. H., et al. (2005), Comparing clouds and their seasonal variations in 10 atmospheric general circulation models with satellite measurements, *J. Geophys. Res.*, **110**, D15S02, doi:10.1029/2004JD005021.
- Zhang, Z., P. Yang, G. W. Kattawar, S.-C. Tsay, B. A. Baum, Y. Hu, A. J. Heymsfield, and J. Reichardt (2004), Geometrical-optics solution to light scattering by droxtal ice crystals, *Appl. Opt.*, **43**, 2490–2499, doi:10.1364/AO.43.002490.
- Zhang, Z., P. Yang, G. Kattawar, J. Riedi, L. C. Labonnote, B. Baum, S. Platnick, and H.-L. Huang (2009), Influence of ice particle model on satellite ice cloud retrieval: Lessons learned from MODIS and POLDER cloud product comparison, *Atmos. Chem. Phys.*, **9**, 7115–7129, doi:10.5194/acp-9-7115-2009.

J. M. Comstock, Pacific Northwest National Laboratory, PO Box 999 MSIN, K9-24, Richland, WA 99352, USA.

A. K. Heidinger, Center for Satellite Applications and Research, NOAA National Environmental Satellite, Data, and Information Service, 1225 W. Dayton St., Madison, WI 53706, USA.

S. Platnick, Laboratory for Atmospheres, NASA Goddard Space Flight Center, 8800 Greenbelt Rd., Greenbelt, MD 20771, USA.

P. Yang, Department of Atmospheric Sciences, Texas A&M University, MS 3150, College Station, TX 77843-3150, USA.

Z. Zhang, Goddard Earth Science and Technology Center, University of Maryland, Baltimore County, 5523 Research Park Dr., Ste. 320, Baltimore, MD 21228, USA. (zzbatmos@umbc.edu)